Ultrasonics Sonochemistry 29 (2016) 104–128

Contents lists available at ScienceDirect

Ultrasonics Sonochemistry

journal homepage: www.elsevier.com/locate/ultson

Review

Sonochemistry: Science and Engineering

Nimesh Pokhrel *, Phani Kiran Vabbina, Nezih Pala

Integrated Nanosystems Research Lab, Florida International University, 10555 W Flagler Street EC 3975, Miami, FL 33174, USA

ARTICLE INFO

Article history:
Received 5 October 2014
Received in revised form 21 July 2015
Accepted 21 July 2015
Available online 26 July 2015

Keywords:
Sonochemistry
Ultrasound
Nanomaterial synthesis

ABSTRACT

Sonochemistry offers a simple route to nanomaterial synthesis with the application of ultrasound. The tiny acoustic bubbles, produced by the propagating sound wave, enclose an incredible facility where matter interact among at energy as high as 13 eV to spark extraordinary chemical reactions. Within each period – formation, growth and collapse of bubbles, lies a coherent phase of material formation. This effective yet highly localized method has facilitated synthesis of various chemical and biological compounds featuring unique morphology and intrinsic property. The benign processing lends to synthesis without any discrimination towards a certain group of material, or the substrates where they are grown. As a result, new and improved applications have evolved to reach out various field of science and technology and helped engineer new and better devices. Along with the facile processing and notes on the essence of sonochemistry, in this comprehensive review, we discuss the individual and mutual effect of important input parameters on the nanomaterial synthesis process as a start to help understand the underlying mechanism. Secondly, an objective discussion of the diversely synthesized nanomaterial follows to divulge the easiness imparted by sonochemistry, which finally blends into the discussion of their applications and outreach.

* Corresponding author.
E-mail address: NPOKH002@FIU.EDU (N. Pokhrel).

http://dx.doi.org/10.1016/j.ultsonch.2015.07.023
1350-4177/

1. Introduction

By virtue of their unique properties that differ significantly from their bulk counterparts, nanomaterials offer novel applications to the field of science and technology. Reducing the size of a material to nanoscale confines the electrons (and photons) inside to limited movement that brings changes to its physical and chemical property [1,2]. Such expedient change have fostered many new applications while improving existing ones. Therefore, the idea to synthesize nanomaterials with desired morphology and applicable property have spurred great interest and technological evolution. From simple solution based methods like sonochemistry, solvothermal, hydrothermal etc., to cutting edge methods like lithography, epitaxy, ablation etc., the diversity in nanomaterial synthesis technique can be exploited to achieve control over growth. Sonochemistry offers a unique control over crystallinity that enables synthesis of amorphous metals and metal alloys. Compared to most methods, sonochemistry is very inexpensive and economical, allowing individual researchers and enthusiasts experience and try ideas. It rose into prominence with the rise in interest in material processing and engineering since past 30–40 years. However, study of chemical reactions and changes in chemical solution with the application of ultrasound dates back to as far as early 20th century [3]. Reports have marveled and helped the field span manifold while arousing researchers and reviewers. Review on sonochemistry, therefore, is not uncommon. However, the common discussion on types of material synthesized and their synthesis route, without focus on the effect of applied parameters on their growth and the advancements they have bought, provide more information and less insight. Our objective is to provide a comprehensive review, bringing together all necessary information to help understand the theory and methods of sonochemistry and its contribution to various fields.

Ultrasound passing through a solution creates regions inside the solution with high and low pressure region according to the periodic compression and expansion [4,5]. This change in pressure marks the inception of sonochemistry, as it precedes the crucial process of acoustic cavitation i.e. formation, growth and collapse of acoustic bubble. Air molecules dissolved in the solution diffuse to form bubbles at the low pressure cycle. On reaching the next cycle, the high external pressure compresses the bubble and the matter inside violently. This process of bubble growth and compression continues until the external pressure dominates and the bubble collapses, as shown in Fig. 1. As they contract, the acoustic bubbles, with high energy particles inside, emit light (200–800 nm) for a very brief period (about 100 ps). This phenomenon, known as sonoluminescence, can be used to analyze the condition inside the acoustic bubble [6–8]. With the help of such tools and theories, pressure and temperature inside the bubble has been calculated to rise to more than 1000 atm and 5000 K during cavitation [9,10]. The core region, known as the hotspot, feature high-energy particle collision that generate energy as high as 13 eV [11]. Extreme cases of ionization and formation of plasma inside the bubble have been reported with different chemicals and solvents [12–14]. Evidence of nuclear fusion during cavitation, though a disputed concept, epitomizes the effect of ultrasound and presents a simple, viable tool to study nuclear reactions [15]. Such conditions can induce abnormal physical and chemical changes and facilitate the very basic reaction between atoms and molecules to produce extraordinary class of materials [16–21]. However, the utility of sonochemistry lies in the fact that the ions and radicals inside the bubble comes from the chemical solution; therefore, choosing appropriate chemicals based on their vapor pressure can help customize the overall process.

In addition to the hotspot energy and associated chemical effects, the acoustic bubbles give rise to useful physical phenomenon during collapse, as shown in Fig. 2. The physical phenomenon arises either from implosion due to ambient pressure or explosion due to boundary. Bubble that reach the boundary explode outwards to produce microjets that offer distinct

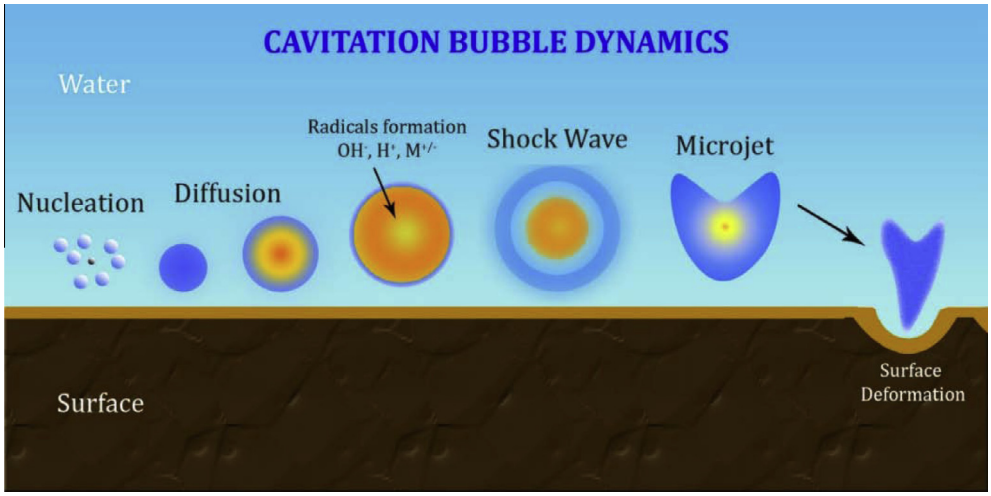

Fig. 1. The process of acoustic cavitation and its effect.

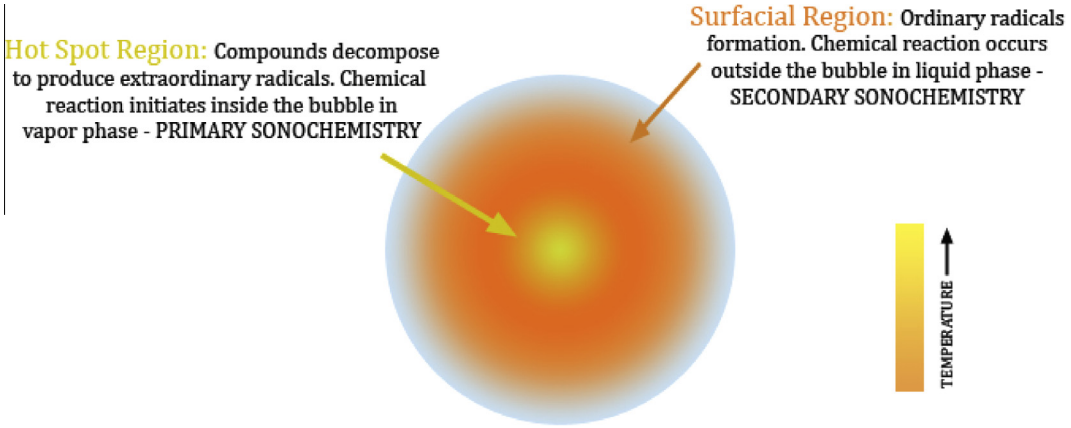

Fig. 2. A vivid representation of different domain inside an acoustic bubble.

applications [22]. Similarly, the imploding bubbles produce shock waves that accelerate undissolved solute and impurity particles to several hundred meters per second [23]. Collision at this speed results in drastic structural transformation and can be used for various purposes. Brittle materials break down to fragments to produce fine particles, a process commonly known as sonofragmentation that has shown to be more effective and benign than ball milling and similar processes. Shock waves may also impact particles directly and induce fragmentation without the need of collision [24]. In addition to fragmentation, the physical effect has also found widespread use in exfoliating layered materials like graphite, boron nitride, molybdenum disulfide etc. to produce their 2D counterparts [25–27]. The distribution of matter and the effect of shock waves and microjets that follows a bubble death only span close proximity, therefore the effect of sonochemistry to the ambience is fairly benign. Such combined, facilitating effects of sonochemistry render the synthesis of delicate and uncommon materials such as protein, liquid microspheres, hollow nanospheres, graphene, fibers etc. and the use of paper, cotton, nylon etc. as substrates [28–34].

The use and study of ultrasound for material processing is a very matured and popular concept. Sonochemistry arose into prominence during the early 80's, when Suslick started wreaking havoc inside solutions with his ultrasonic machine gun [35–38]. Nanostructures with unique physical and chemical property have evolved to lend new and improved applications across multiple fields [39–45]. The sincere devotion of sonochemists has immensely helped in upbringing of this field and to make it as diverse and vastly applicable, while maintaining the simplicity intact. The simplicity lies in the cavitation process itself that merely involve the evolution of a bubble but embodies the overall sonochemical process. Hence, understanding acoustic cavitation and its underlying variables becomes vital in comprehending sonochemistry and its applications. This review paper is structured accordingly. The upcoming theory section explains the cavitation mechanism as a whole, addressing the effect of various input parameters that influence cavitation and the material formation process, which comes naturally. Knowing this basic phenomenon, one gains necessary intuition of the mechanism behind the synthesis of different metal and semimetal compounds, which is explained individually in the following section. The advancements section, the final section, presents the current uses of sonochemistry and sonochemical nanomaterials in the field of sensing, photovoltaics, magnetics and storage, catalysis, biomedical engineering etc., focusing more on improvements and advantages imparted and novel applications engendered. To start, a brief introduction on the study of cavitation follows.

2. Theory and Discussion

Acoustic cavitation is an interesting phenomenon, and interestingly, its study was first conducted for its detriments rather than its possible application. Lord Rayleigh derived a preliminary notion of the subject on being summoned to examine damages to the propeller of HMS Daring (1893). Coming up with the idea of associated cavitation by sonic waves, he deduced a mathematical model for the formation of cavities inside a liquid, and predicted the existence of hot spot inside the bubbles back in the 19th century [4,6]. Given in the Ryleigh Eq. (1), the size and growth of bubble should reciprocate the pressure change. Although this equation discards the effect of viscosity and surface tension, which Plesset included in his Rayleigh–Plesset Eq. (2), it serves as a basic model for acoustic cavitation:

$$R\ddot{R} + \frac{3}{2}(\dot{R})^2 = \frac{(p - p_o)}{\rho} \tag{1}$$

$$R\ddot{R} + \frac{3}{2}(\dot{R})^2 + \frac{4\sigma\dot{R}}{R} + \frac{2S}{\rho R} = \frac{(p - p_o)}{\rho} \tag{2}$$

where R is the radius of the bubble and is a function of time, ρ is the density, σ is the viscosity and S is the surface tension of the liquid respectively and $p - p_o$ is the pressure difference between compression and rarefaction cycle. The pressure difference can be calculated using simple wave equation as shown in Eq. (3).

$$P(x,t) = A\cos(\omega t - \beta x + \varphi) \tag{3}$$

Here, A, ω, β and φ denote the amplitude, frequency, wave number and reference phase of the sound wave respectively. The amplitude and frequency determines the magnitude and rate of oscillation of the pressure field, and is critical to the formation and sustaining of acoustic bubbles. The pressure decreases at rarefaction, such that the local temperature becomes sufficient for dissolved air bubbles and edge cavities to diffuse, a process known as rectified diffusion [1,11]. Since tensile strength of liquid is extremely high, the possibility of cavity formation from acoustic expansion due to ultrasound can be simply ignored. During rectified diffusion, air cavities nucleate around a particle or conglomerate to form bigger cavity – a sub process known as nucleation. The diffusion process completes within a rarefaction cycle and leads to the oscillating growth of the bubble. After rarefaction, the new born bubble is squeezed and shrunk by the external pressure that tries to implode it. To further cavitation, the bubble overcomes this high pressure cycle by adapting a suitable size. Depending on the applied amplitude and frequency, the size increases from few

micrometers to hundreds of micrometer between the inception and final phase within milliseconds [46,47]. As the bubble reaches the compression at its peak, the external pressure dominates and the bubble implodes. The dying bubble is reduced instantaneously to ~10th of its size before implosion; while the matter inside turns to plasma due to the violent compression [26]. Filled with extraordinary ions diffused by the decomposing chemical solution, the energy inside the bubble can rise to as high as 13 eV from inter-ion collision [10–12,22]. This hotspot energy is conferred to the ambient liquid along with the ions and chemicals upon bubble implosion. Additionally, the imploding bubble produces shockwave during the collapse that entail high acoustic streaming and mass transfer [9,10]. Bubbles near the boundary however die untimely with an explosion as they are devoid of the freedom to move and grow. These bubbles taper as they get pushed to the wall and ultimately explode in an asymmetrical fashion. Compared to shock wave and the availing physical effect of implosion, the exploding bubbles give rise to high speed jet of liquid that produce surface deformation, erosion and similar undesired effect. Moreover, such premature cavitation rarely form hotspot, therefore serve very less to the purpose of sonochemistry. The sonochemical efficiency is therefore a function of implosion i.e. cavitational collapse, a dynamic variable that incorporates the effect of homogeneity and similar applied parameters.

Homogeneous solutions benefit inclusively from the applied ultrasound as physical and chemical effect work in concert towards material synthesis. In case of heterogeneous mixture and slurry, the physical effect becomes dominant – small particles driven by shock wave undergo drastic structural transformation upon collision while bigger particles participate in shock wave induced collisions and additionally give rise to microjets due to boundary effect. On the other hand, small particles can also feature as nucleation center and undergo successful cavitation to fracture itself, thereby producing fine nanoparticles [48]. As such phenomenon is random and uncontrolled, without a standard model to study its impact, deriving application from physical/heterogeneous sonochemistry is hitherto indefinite; but growing. However, in case of homogeneous solution, the physical effect is nominal and subsidiary, which makes the system easier to analyze and study. In other words, homogeneous sonochemistry roots on cavitation than its aftereffects, and therefore is simple, efficient and more popular. Being a solution-based method, homogeneous sonochemistry also benefits from the dissolution of organic precursors that breakdown into intermediate compounds before sonication. The primary breakdown favors the desired entropy change and enables the use of other low energy, solution based methods such as hydrothermal and solvothermal for nanomaterial synthesis. Sonochemistry extends this natural process and offers a facile and unique way to achieve incredible energy and changes with the application of ultrasound.

Ultrasound wavelength is large compared to the dissolved species, therefore physical and chemical changes associated with sonochemistry due to wave-particle interaction is mostly incoherent. Dissolved compounds in the micrometer scale can however form the bubble core during diffusion and experience firsthand the effect of ultrasound through cavitation. The primary reaction taking place inside the bubble in this case is between precursor ions and other chemicals. This type of sonochemistry where precursors participate to form hotspot, known as primary sonochemistry, produce extraordinary class of materials. The part of material formation comes into play as the magma of matter erupts into the ambient solution after implosion. The hot matter quenches and solidifies instantly as it comes in contact with the solution, while cooling at a rate as high as $\sim 10^{10}$ K/s [10,22]. The following shock wave facilitates the cooling process as it distributes the bubble content with a far-reaching outward blast. The combined chemical and physical effect produces fine nanostructures with unusual shape, size and natural property. Secondarily, the scattered ions and radicals interact with the solution and instigate chemical reactions to give rise to another sonochemical route to material synthesis, known as secondary sonochemistry. Materials formed in this way are products of chemical reactions taking place outside the bubble free from an imposing physical force; therefore feature properties similar to their normal nano-counterparts. The significance of sonochemistry, as a result, lies in its primary form where energy and matter interact in a flowing condition to produce extraordinary materials.

Organometallic compounds are commonly used as sonochemical precursor. These compounds dissolve fluently in common solvents like water and alcohol to produce intermediate metal compounds and are volatile that facilitates primary sonochemical reaction. The volatile metal can vaporize from local heating and undergo a successful cavitation. With the wide range of available precursor and solvent, the freedom to choose and combine one based on volatility and relevant property can be simply used to customize the bubble i.e. sonochemistry as a whole; as matter inside the bubble determines the oncoming reactions. This freedom therefore presents a tool to help lead a desired route to material formation and improve process yield. The use of nonvolatile precursor, however, may not be able to replicate similar physical condition and trigger a direct reaction. In such case, the solvent, being more volatile, undergoes cavitation and produce reactive chemicals, like H^+/OH^- ions in case of water that react with the dissolved precursor and instigate synthesis reaction. In addition to the diffusing solvent, dissolved gases such as CO_2, O_2, NH_3, CH_4 etc., added surfactant and/or similar agent can participate in cavitation and breakdown to react with the precursor. In this way, different chemicals can be brought into play as to direct the synthesis reaction per need. Quite fairly, primary sonochemistry provides good physical condition for chemical reactions but secondary sonochemistry allows more chemical route to synthesis.

The ability to architect sonochemistry with relevant chemical, solvent, frequency, amplitude etc. is a handy resource to researchers. It is therefore wise to venture into knowing the impact each field – frequency and power of ultrasound, time of experiment, nature and concentration of solution etc. have on the overall process [49–51]. Only upon gaining the necessary intuition can a clear and analytical mind be set to logically understand the materials formed. Therefore, we have put a brief and separate chapter of each applied parameter and its individual and mutual effect on cavitation and material synthesis.

2.1. Effect of Solution

Solution as a whole incorporates various sonochemical ingredients such as precursor, solvent, additives and chemical agents, dissolved gas etc. [21,52–57]. Changing one of them can solely bring new and remarkable changes on the process. Among these applied solution parameters, the effect of solvent, in particular, is of imperative value. It carries the combined effect of viscosity, vapor pressure and surface tension that can be associated with each sonochemical stage: pressure buildup, diffusion and bubble growth [56,58]. The effect of viscosity reflects on process yield while vapor pressure can be as instrumentation as to divide sonochemistry into primary and secondary like discussed before. Solvents with low surface tension help the bubble reach a suitable size and stabilize, even though it entails a reduction in cavitation intensity due to increased growth and growth density. Addition of solute concomitantly decreases the surface tension that can be further decreased with the inclusion of surfactants [56,59]. Such

chemicals can also be used to prompt new chemical reactions as a means to obtain new materials, as a stabilizing, growth directing agent or simply to study their effect on cavitation [56,59–66]. Use of electrolytes has shown to inhibit bubble coalition and enhance single bubble sonoluminescence. The electrolyte at the bubble interface creates an electrostatic repulsion between bubbles that help them grow solely; which also increases their resistance to compression. Nanomaterials with unusual shape and crystallinity, improved physical and chemical property has been achieved as a result [67–70]. Atomic level mixing inside the bubble provides alternate, possibly low-energy, route for chemicals to form new materials or improve existing ones in terms of their stability, reactivity etc.

Increasing precursor concentration has shown to produce similar results in terms of bubble coalition and single bubble sonoluminescence [71]. The change in precursor concentration, as a result, affects morphology of nanoparticle during growth [21,52,70]. In a typical case of ZnO synthesis, the shape of ZnO changed from 1D nanorods and nanowires to 2D nanosheets, nanocups, nanoflakes etc. on increasing precursor concentration while keeping other parameters constant. In absence of other chemicals, increasing precursor concentration shows to favor growth along multiple axis. The amount of gas dissolved in the solution shows similar effect on sonoluminescence but no significant effect on bubble coalition [57,61]. Subnormal gas content, degassing and use of old solution hinders the ability of liquid to cavitate and consequently reduces sonochemical yield.

2.2. Effect of Frequency

The effect of frequency reflects on the pressure cycle. On increasing frequency the pressure changes abruptly, causing high turbulence inside the liquid. This induced effect, known as acoustic streaming, dominates acoustic cavitation at high frequency and amplitude [5]. Due to streaming, bubbles get pushed and harried constantly and die immaturely, resulting in poor cavitation and material growth. In addition to the effect from streaming, the development of cavitating bubble is impeded by the reduced diffusion time during high frequency experiment. Increasing the frequency shows to produce bubbles with small size and uniform size distribution [72,73]. However, the energy building up inside the bubble do not reciprocate the increment in frequency as linearly as the changing size. Analyzing the formation of different hydrocarbon compounds during sonication of aqueous tert-butyl, temperature inside the bubble was calculated in the range of 3400 K at 20 kHz, 3700 K at 1056 kHz, and highest of 4300 K at 355 kHz [74]. The rate and type of radical formation as a result changes with frequency such that primary radicals and ions are produced during certain frequency range, in other words it is impractical to assume extreme cases such as O_2 ionization at any frequency and power [72]. Theoretical calculation, simulation and sonoluminescence study of the effect of frequency show that the cavitation process is enhanced during a frequency range that depends on the type of solution used [72–74].

The effect of frequency on cavitation consequently affects the material synthesis process. Okitsu et al. assessed the formation of gold nanoparticles under varying ultrasonic frequency by analyzing the rate and size of gold nanoparticles [51]. The study conducted by sonicating an aqueous auric chloride and 1-propanol solution at constant power and temperature showed that the rate of formation of gold nanoparticles increases linearly from 0 to 213 kHz, peaks at 213 kHz, and decreases smoothly. TEM results showed that the size of nanoparticle decreases with frequency with smallest gold of ~10 nm obtained at the peak frequency. To evaluate sonochemical efficiency with respect to frequency, Koda et al. performed a study on Fricke reaction, KI oxidation and decomposition of porphyrin derivatives under the frequency range of 19.5–1200 kHz [75]. Using individual reaction system and with the help of calorimeter and UV spectrometer, the formation of free radicals in each system was analyzed. In all cases, the rate of reaction and formation of Fe^{3+} (Fricke), I_3^- (KI oxidation) and H_2TPPS^{4-} (porphyrin decomposition) radicals was significant at the frequency range of 100–500 kHz, optimal at ~300 kHz. From various experiments, the favorable frequency for efficient cavitation and nanomaterial growth has been found to be in the range of 100–400 kHz [51,72–75].

2.3. Effect of Power

The applied power i.e. power density reflects on the pressure amplitude and should be able to supply the pressure need for cavitation. Increasing power drastically can however disrupt bubble dynamics as it helps bubbles grow abnormally during expansion that may result in poor cavitation and material growth [72,73]. Therefore, the applied power and frequency should always correlate in order to balance the bubble growth. For the standard water based experiment, at 20 kHz ultrasound frequency, the average bubble size measured at a distance 30 mm below the transducer, at an input power of 179 W (P_d = ~62.153 KW/m^3) was found to be ~10 μm [46]. The size of bubble, in general, shows to increase with applied power at frequency 500 kHz or below [73]. At high frequency, however, increasing power above certain level induces nonlinear effect on bubble growth. In a typical case (1056 kHz), increasing power from 0 to 5 W resulted in an increase in bubble size from ~1.8 μm to ~4 μm, while increasing the power further (5–30 W) showed a wavering growth pattern that produced a change of ~0.8 μm [73]. The effect of increasing power under varying frequency reciprocates similarly – between 200 and 300 kHz, bubble growth with respect to power and frequency was found to be linear, but for 500–1000 kHz a quasi-linear relationship was observed, and for 1000 kHz and higher, increasing power decreased the bubble size [72]. Such adverse effect at 1000 kHz can be attributed to acoustic streaming caused by high frequency and power.

The type of radicals formed changes accordingly with respect to applied power as in the case of frequency and induces conspicuous changes on the morphology and crystallinity of nanomaterials [50,72,76]. The size of nanoparticles shows to decrease with power while the sonochemical yield increases. ZnO nanoparticles showed interesting changes, producing distinct shape and size with respect to the power change – flakes were prevalent at 12 W while rods dominated the growth at 21 W and spheres at 45 W. Maintaining a low temperature was helpful in synthesizing smaller nanoparticles and minimizing byproduct formation [50].

2.4. Effect of Sonication Time

The effect of time of experiment and number of cycle induces morphological variation in nanomaterials formation [21,77–79]. With increasing time and cycle of sonication, formation of new structures is made easier by the primary growth that serve as seed. Depending on the surface energy, new heterostructures build on top of existing ones. In case of ZnO synthesized via sonication of aqueous zinc acetate dihydrate, zinc nitrate hexahydrate and hexamethylene tetramine, the time of sonication reflected apparent changes on the morphology of ZnO nanomaterial formed, as shown in Fig. 3 [21]. In a more specific case, MoS_2 synthesized via sonication of molybdenum hexacarbonyl, sulfur and o-xylene, transformed from 2D nanoflakes to 3D nanospheres, like organic fullerenes, while sonicating for an extended time [78]. The

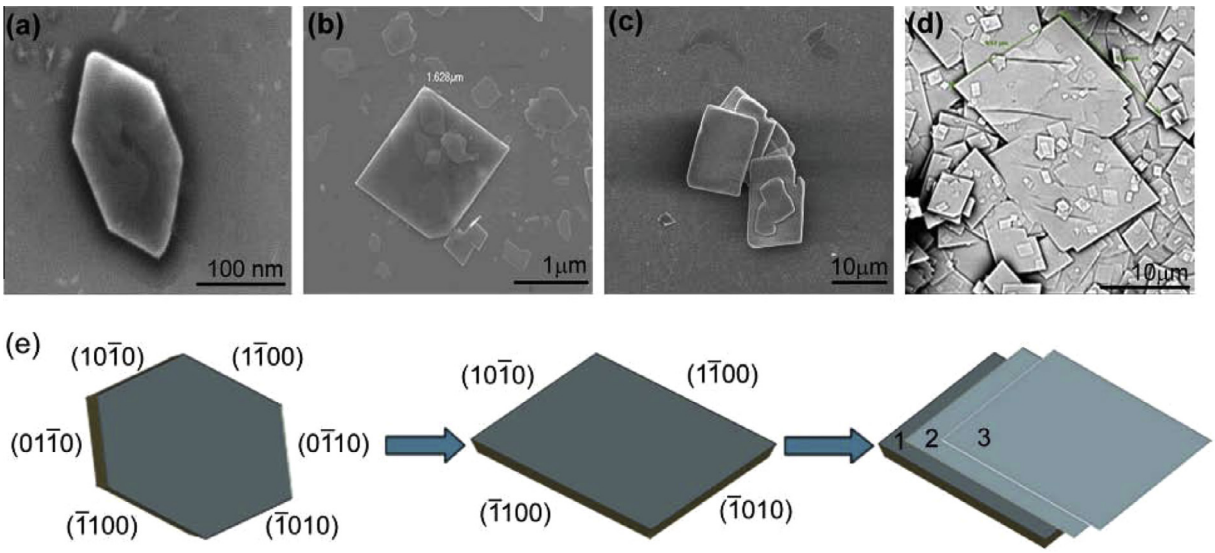

Fig. 3. Change in shape of ZnO nanoparticles with respect to sonication time: (a) 1 min (b) 3 min (c) 15 min (d) 30 min. (e) Transformation of hexagonal shape to parallelogram and parallelogram-stack. Reprinted with permission from [10].

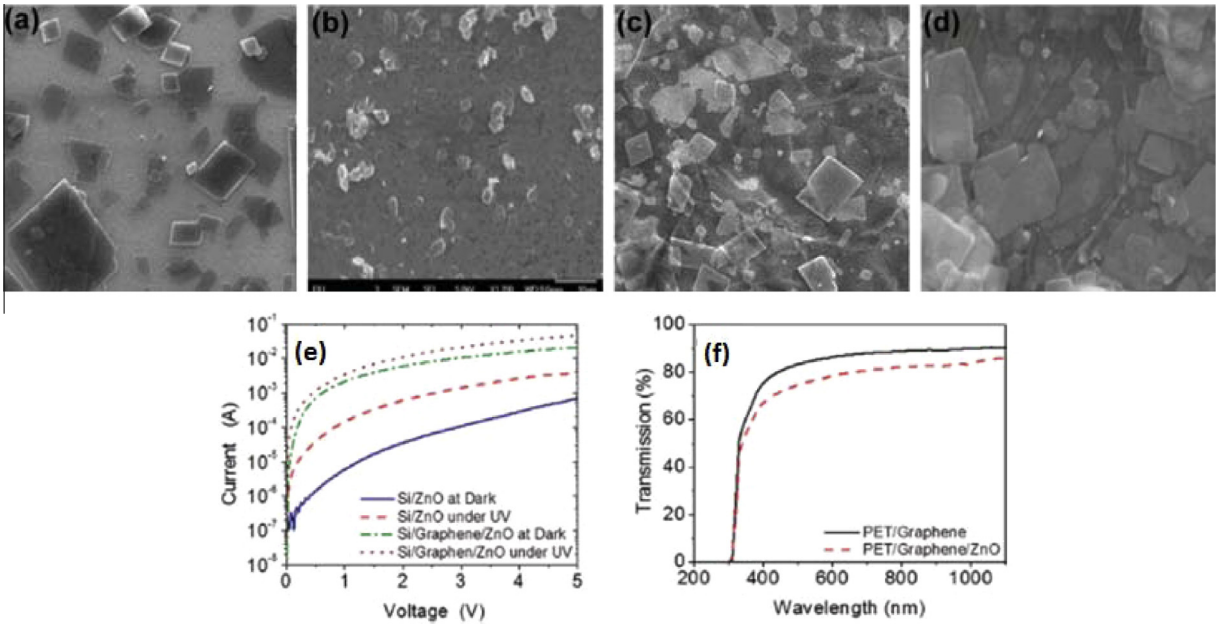

Fig. 4. Effect of substrate: (a) SiO_2 (b) graphene/Si (c) graphene over SiO_2 (d) graphene over PET (e) compared to ZnO–SiO_2, the conductivity of ZnO–graphene is 10 times higher (f) difference in optical transmission. Reprinted with permission from [10].

increased sonication can also affect the crystalline structure of the product. Stibnite nanoparticles synthesized sonochemically changed from amorphous nanospheres to crystalline nanorods and nanowhiskers upon prolonged sonication [79].

2.5. Effect of Substrate

Choice of substrate produces striking morphological changes in nanomaterials grown atop in addition to bringing changes to their electrical, chemical and other properties [21,80,81]. As demonstrated by a chitosan modified ITO glass substrate, the synthesized Au–Pt nano composite on chitosan surface grows much smaller and denser compared to the ones grown on bare ITO [80]. Similarly, ZnO grown on graphene coated substrates showed higher growth rate and density compared to bare SiO_2 and PET substrates, as depicted in Fig. 4 [21]. Upon prolonged sonication, ZnO on graphene formed 3D nanostructures useful for applications requiring continuous transport medium [87], contrary to the formation of 2D nanoflakes on bare SiO_2. Additionally, the photoconductivity of ZnO grown on top of graphene compared to Si increased substantially, and is shown in Fig. 4(e). In case of noble metals, choice of substrate plays a vital role in enhancing their sensing and catalytic property [81]. Size, orientation, density etc. of such nanometals that affects their property relies on the surface where they are grown; and use of substrates such as: graphene, CNT, chitosan etc. with high-surface area has proved to improve their growth and features.

2.6. Physical Effect of Ultrasound

As sonochemistry basically pertains to the chemical effect of ultrasound, we have dedicated this section to discuss the effect of shock waves and microjets and applications derived from them. The effect of shockwave is more prominent than microjet and can induce diverse structural changes – brittle material break down to fragments, ductile materials deform while layered materials exfoliate [23,25,82,83]. Zinc, iron, tin, chromium and similar transition metal microparticles (~50 μm) show to form dumbbell-like structures upon sonication of their respective slurry [23]. However, sonicating a slurry of nickel micro particles (~160 μm) showed very low interparticle coalition due to the large size. Increasing the particle size increases the drag and consequently decreases the kinetic energy generated by shock wave acceleration. The temperature at the collision point can reach as high as 2890 K, as evidenced by coalition between molybdenum particles [23]. Metals with low melting point coalesce while the ones with high melting point fragment. Tungsten micro-particles expectedly showed no significant physical change upon sonication [23]. The exfoliating effect of ultrasound has become more popular among sonochemists due to its potential application in synthesis of graphene and similar contemporary materials. Reports demonstrate significant improvement in the physical and chemical property of sonochemically prepared graphene compared to conventional methods [26,29,30]. Graphene exfoliated from graphite flakes as reported by Xu et al. show majority of graphene with less than 5 layers and with very low surface roughness and damage [26]. Similarly, Lisa et al. report a novel method to prepare carbon nanoscrolls by exfoliating graphite with the help of alkali metals and ultrasound [25]. Additionally, synthesis of single to few layers molybdenum disulfide (MoS_2), tungsten disulfide (WS_2) and boron nitride (BN) has also been simplified by ultrasonic exfoliation [84]. In addition to interparticle collision, shockwave can interact directly with particle of suitable size and induce fragmentation [24]. Eliminating other means of collision, Zeiger et al. report the effect of coupling between aspirin crystal and shock wave that lead to fragmentation [24].

Contrary to shockwave, the effect of microjet is perturbing to sonochemists as the rushing jet produces undesired effect such as surface erosion, pitting, deformation etc. The effect of microjets can however be controlled and utilized for many applications such as cleansing, activation of metal, catalysis, drug synthesis etc. [38,85]. For activating metal and reactive compounds, microjets remove oxide and other surface coating easily and thoroughly, offering a better alternative to heating and conventional methods [38]. Microjets have also found its use in engineering – Barton et al. report the fabrication of microelectrode array sensor via controlled pitting [86].

3. Synthesis and Application

The type and class of materials synthesized sonochemically has become so extensive that reviewing one class will fill in a review. In this section, we have therefore categorized their synthesis into respective group to make the information easily accessible. This helps reader understand the process similarity and us to focus on their importance and applications. The mechanism for sonochemical synthesis corresponds to the chemical effect of ultrasound, except for cases where the physical and chemical effects act simultaneously. With the inherent understanding of chemical bond and bond formation and dissociation, the underlying chemical reactions for the formation of a material is easy to grasp. This basic understanding makes the sonochemical process easy to analyze and improve.

While other methods ask for high temperature, pressure and strict conditions to be fulfilled in prior, inevitably complicating the process, sonochemistry elegantly makes use of the availing conditions entailed by the process. On top of being efficient, sonochemistry is affordable, convenient and runs economical. A typical sonochemical setup consists of an ultrasound probe and a signal generator as shown in Fig. 5. The ultrasound probe (Fig. 5A) when dipped into the solution and activated with a source (Fig. 5B) sets up the flowing condition for material synthesis naturally. Series of chemical reaction precedes the formation of a nanomaterial, the nature of which depends on the participating reactants. High vapor pressure precursor when used in concert with low vapor pressure solvent help the precursor undergo primary sonochemical reactions and improve sonochemical yield [22]. Upon implosion, the matter inside, in such case, is cooled at an incredible rate of $\sim 10^{10}$ K/s, due to which it solidifies before crystallizing [7,16]. Therefore, by simply analyzing the crystallization of product, one can surmise the type of sonochemistry that underwent as well as get an understanding of the precursor vapor pressure with respect to solvent. A synthesis reaction between tungsten hexacarbonyl and diphenylmethane (DPhM) for the formation of tungsten carbide is shown in Eqs. (4)–(6) [87]. The low vapor pressure of DPhM helps in the primary decomposition of tungsten hexacarbonyl. The thus liberated metal forms metal nanostructures via self-assembly or combine with other chemicals produced during sonication to form metal compounds. This process depends on the detached metal – (1) whether it is an atom or ion, which is also influenced by the type of its precursor bond, and essentially (2) the ability of such metals to form a stable metal structure by itself.

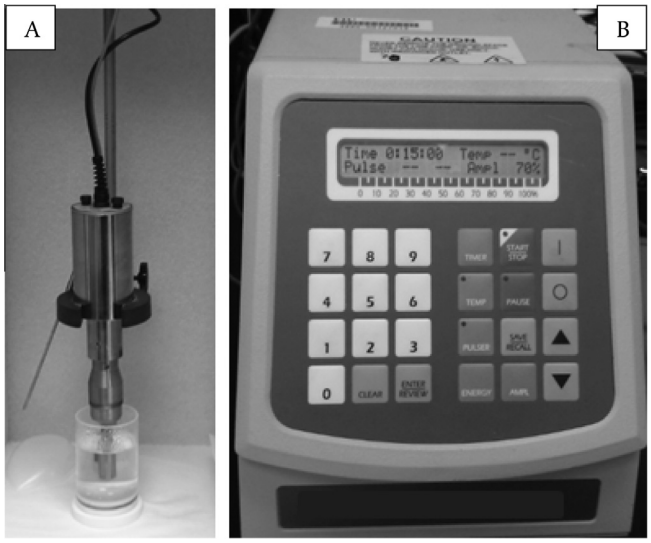

Fig. 5. A simple sonochemical setup for nanomaterial synthesis.

$$(C_6H_5) - CH_2 - (C_6H_5) \longrightarrow C_2H_2 + CH_4 + H_2 \quad (4)$$

$$W(CO)_6 \longrightarrow W + 6CO \quad (5)$$

$$W + C_2H_2 \longrightarrow WC_X + H_2 \quad (6)$$

The formation of oxide, carbide etc. can be useful, as most metal nanoparticles are unstable and volatile in nano form. However, formation of such compounds limit the reactivity of metal nanoparticles desired for many applications and may require post processing such as annealing, purging, chemical washing etc. To overcome the natural instability and preserve their applicable property, chemical stabilizers can be used, and is quite popular in sonochemistry [68,88]. The decomposing organic solvents, in some case, itself forms a protective layer on top of metal and helps the product stabilize. Methane derivatives and similar compound, as shown

Table 1
List of commonly used chemicals for sonochemistry and their physical characteristics – vapor pressure data corresponds to measurement at 25 °C except for DPhM (at 151 °C) [35–37,90–92].

Low vapor pressure	Property	Primary compound/radical	High vapor pressure	Property	Primary compound/radical
Dimethylformamide	B.P. ~150 °C, V.P. ~498 Pa	Amine $C_2H_6{-}N^-$	Acetone	B.P. ~56 °C, V.P. ~30.6 kPa	Methane CH_3^-
Decane	B.P. ~174 °C, V.P. ~195 Pa	Alkane $C_NH_{2N+1}^-$	Ethanol	B.P. ~78 °C, V.P. ~25 kPa	Hydroxide OH^-
Diphenylmethane	B.P. ~298 °C, V.P. ~3.9 kPa	Alkyne $C_NH_{2N-3}^-$	Isopropanol	B.P. ~83 °C, V.P. ~5.3 kPa	Hydroxide OH^-
Isodurene	B.P. ~197 °C	Alkane $C_NH_{2N+1}^-$	Carbonyls	B.P. ~103 °C (Iron)	Methane CH_3^-

in Table 1, formed due to sonolysis of solvent can form surficial bond with the active metal and develop a thin protective enclosure [36]. For the option of various stabilizing and growth directing chemical agents and solvents, the increasing sonochemical control has helped obtain nanoparticles with desirable physical and chemical properties [69,90,91].

3.1. Metal Compound

Transition metal and metal compounds are popularly synthesized as they possess good electrical, magnetic and other applicable properties, are easy to synthesize and are of good commodity [93–97]. Metal carbides synthesized from their carbonyl precursors are generally amorphous while metal oxides synthesized from acetates are crystalline. The transient nature of cavitation also helps such amorphous metal and metal compounds grow in porous form and achieve high surface area, which enhances their absorption, useful for catalysis, sensing and other applications [18–20,89,98,99]. Oxygen incorporation and excess carburization during the synthesis process, however, can destroy the catalytic property of such metal nanoparticles [18,19]. In order to prevent contamination, the sonochemical process is carried under an inert gas flow followed by controlled annealing in a closed and inert system [18,87]. The annealing process induces crystallization and agglomeration that may result in higher particle size, but essentially improves the overall stability of metal nanoparticles.

Organic solvents such as DPhM, decane, isodurene etc. is commonly used for synthesis of metal and metal compound nanoparticles. Compared to decane and durene, DPhM can also function as a growth capping agent in addition to a carbon reagent [87]. As a result, sonicating $W(CO)_6$ and DPhM produces fine, well dispersed and unagglomerated W_2C nanoparticles [87]. Sonicating the $W(CO)_6$ and DPhM solution in presence of oxygen, however, results in the formation of tungsten oxide (WO_2) nanoparticles instead of W_2C [115]. Similarly, adding sulfur to the $W(CO)_6$ and DPhM solution changes the product from W_2C to tungsten sulfide (WS_2) [116]. The ability to change the result as drastically with a slight tweak exemplifies the ease sonochemistry offers to the synthesis of metal nanomaterials.

3.1.1. Metal Carbide

Metal carbide nanoparticles, popular for their catalytic applications, synthesized sonochemically from their carbonyl precursor possess high chemical and physical stability [44]. Tungsten and molybdenum carbide nanoparticles are popularly used as an economical alternative to platinum and ruthenium for their similar catalytic properties [20,97,100]. Commonly used for dehydrogenation of organic compounds, sonochemically synthesized molybdenum carbide nanoparticles powder show excellent selectivity towards alkanes over a wide range of temperature. As reported by Hyeon et al., the sonochemical Mo_2C sample activated the C–H bond of cyclohexane without hydrogenolysis – a challenging test for non-platinum catalysts and produced comparable results to commercially available ultrafine Pt and Rh powder [18]. Absence of carbon and coke deposits in the end product alludes to a deactivation-free catalysis, unlike in Pt and Rh based dehydrogenation [101]. Such prominent catalytic property can be attributed to the process that produces ultrafine Mo_2C nanoparticles (2 nm – TEM) with high surface area (188 m^2/g – BET) in the form of porous clusters that enhances chemical absorption. Unlike methods that require multiple step, long processing time, use chemical stimulants etc., sonochemistry imparts an appealing simplicity to the metal carbide synthesis process [102–104].

Metal carbide nanoparticles are also used for dehalogenation, essentially to mitigate the severe effects of chemicals such as CFCs, chlorophenols, chlorobenzenes etc. [100,105]. Catalytic hydrodehalogenation (HDH) has shown to be easier, safer and more efficient than conventional processes such as activated carbon absorption, incineration, catalytic oxidation etc. [105–107]. However, inability of conventionally synthesized metal carbide nanoparticles and commercial catalytic metals to overcome deactivation due to residual effect and their dehydrogenation tendency limits the potential of HDH [15,16]. Sonochemically synthesized Mo_2C and W_2C nanoparticles feature high surface area that can simultaneously dissociate higher number of carbon-halogen bonds to prevent deactivation [100]. As reported by Oxley et al., sonochemical Mo_2C and W_2C sample show little to no dehydrogenation and produce simple organic compounds upon dehalogenation of aryl halides [100]. The result provide potential boost to metal carbide based HDH process over conventional Mo_2C and W_2C nanoparticles and common catalysts such as Pt, Pd, Rh and Ni [100]. In a different note, ultrasound can be applied directly to organic halide solution to induce dehalogenation via sonolysis without the need of physical catalysts; and is widely used in water treatment, dechlorination, environment remediation and similar processes [108–114].

Compared to other transition metals, magnetic transition metal carbide nanoparticles are commonly used in ferro-fluids, sensing, magnetic storage, magnetic hyperthermia, magnetic resonance imaging etc. in addition to catalysis and chemical modification [117–120]. Carburization and carbon coating not only helps stabilize these ferromagnetic nanomaterials, which are naturally pyrophoric in nano form, but also prevents them from inter-magnetic coupling [117,121,122]. Moreover, metal carbide possess high magnetization and magnetic susceptibility compared to metal oxide desirable for magnetic applications [117]. Therefore, formation of carbide is useful, and can be achieved along the process with sonochemistry that otherwise requires long processing time, stringent conditions and chemicals, post treatment etc. [98,121–125].

Iron, for its highest magnetization and expedient magnetic property, bear especial significance in soft-nanomagnet based applications. Pure and stable iron carbide can be simply synthesized by sonicating the commonly available iron carbonyl precursor in an oxygen-free solvent such as DPhM [98,121,122]. The as-synthesized carbide from carbonyl feature small amount of iron oxide due to the participating oxygen coming from precursor decomposition. The oxide can however be removed completely by heating the sample to 1073 K, which ensues important changes to its magnetic property and air resistance [121]. Nikitenko et al. report on a thorough study of the changing physical, chemical and magnetic property of iron carbide nanoparticles synthesized from iron carbonyl with respect to changing temperature [98].

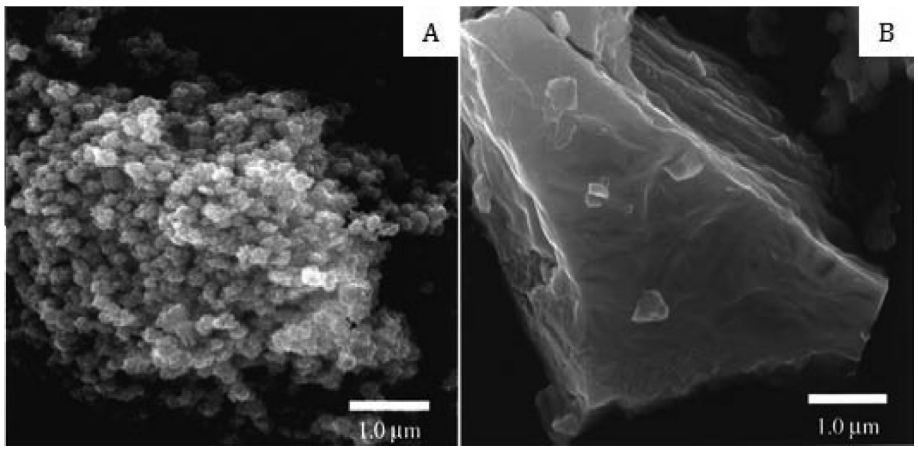

Fig. 6. SEM images of MoS_2 nanoparticles prepared from (A) sonochemistry (B) thermal decomposition. Reprinted with permission from [20].

Annealing performed in an inert environment stabilizes the sample and gradually removes oxygen and other impurity. The as-prepared amorphous and super paramagnetic iron carbide grew in size, stability and its natural ferromagnetic property with heat as it sintered and crystallized. (1) The structure of samples annealed at 973 K and higher featured a core–shell geometry consisting of an iron carbide layer (~5 nm thickness) on top of a crystallized iron core. (2) The magnetization value of the core–shell nanoparticle at 1073 K increased to an extent higher than the point where a bulk iron saturates magnetically. Property (1) and (2) is ideal for applications such as drug delivery, magnetic hyperthermia, ferro-fluid etc. that require high control and responsivity from well-dispersed magnetic nanoparticles. To simplify such applications, the need of purification and high temperature annealing can be obviated with the use of oxygen free iron precursors. Miyatani et al. report on the use of ferrocene/DPhM solution presents an improved alternative to iron carbide synthesis [125]. The ferrocene based solution produced fine iron carbide nanoparticles ~10 nm composed of iron carbide and alpha iron, and showed no trace of oxygen. Similarly, ultrasonication of nickel carbonyl produces amorphous, paramagnetic nickel nanoparticles comprising of carbon and oxygen [17]. The high toxicity of nickel carbonyl however forbids its use and calls in the need of precursors such as nickel acetylacetonate, nickel cyclooctadiene etc. for sonochemistry [126,127]. Sonication of nickel cyclooctadiene has shown to produce an oxide-free, nickel based amorphous compound comprising of nickel and carbon in near equal proportion [126]. The as-synthesized carbonaceous compound produced poor magnetic response that gradually improved with annealing as it crystallized while morphing into a core–shell structure. Due to the chemical inertness, nickel and cobalt do not readily react to from carbide and similar compounds, therefore their sonochemical synthesis is particular and limited.

3.1.2. Metal Oxide

Compared to carbides, nitrides and other metal compounds, sonochemical synthesis of metal oxide has been more diverse in terms of the variety of metal as formation of oxide is easy and common [41,68,69,88,89,99,128–135]. The broad synthesis is mainly driven by the availing properties of oxide nanoparticles that render vastly useful applications across multiple fields [69,88,89,94,136,59]. Metal oxides are generally synthesized from their acetate precursor [41,68,135,137]. In most sonochemical case, the low vapor pressure metal acetate is dissolved in water to form a homogenous solution, which upon sonication, produces crystalline metal oxide nanoparticles. Contrary to hydrophobic metal carbonyls, the secondary oxygen ion in acetates' carbonyl group enables easy dissociation of metal from metal acetate when dissolved. As a result, the homogeneous metal acetate solution enables the use of low energy methods such as hydrothermal, solvothermal etc. [93,135,138]. The slow synthesis reaction taking place in liquid phase allows molecules sufficient time to crystallize.

Kumar et al. report the synthesis of ZnO, CuO, Co_3O_4 and Fe_3O_4 nanoparticle crystals from respective acetate compounds in varying solution [41]. The ionic metal acetate undergoes chemical breakdown in a homogeneous solution depending on the solvent property. In order to investigate the changing chemistry, the growth mechanism was studied for each metal using two solvents: (1) DI water and (2) dimethylformamide (DMF) and 10% DI water, by analyzing the morphology and yield. The similar aprotic polarity of DMF to water allows easy and alike dissolution of metal acetates, however its low vapor pressure reflects on the cavitation process inducing apparent changes to nanoparticle morphology. The DMF based product, however crystalline, featured nanoparticles with smaller size and higher surface area compared to the ones synthesized from water. Addition of chemical agents and stabilizers can strike similar morphological variation [88,68]. CuO nanoparticles synthesized via sonication of copper acetate monohydrate and DMF in presence of polyvinylalcohol (PVA), embed into the polymer and show distinct morphological variation based on the amount of PVA used [68]. In a different case, use of polyvinylpyrrolidone (PVP) alongside urea/sodium hydroxide, changed the crystallization pattern of CuO nanoparticle while changing the reducing agent, as shown in Fig. 7 [88]. These CuO nanoparticles possess valuable chelating feature in addition to the common catalytic property.

In addition to catalysis, iron oxide nanoparticles are known for their magnetism based applications. The profuse availability of organometallic iron helps the synthesis of iron oxide in desired crystalline or amorphous form. Sonicating iron carbonyl produces amorphous Fe_2O_3 nanoparticles, while use of inorganic precursors such as iron ethoxide can help obtain them in amorphous and mesoporous form [69,89,139]. Such form, in addition to their high surface area ~274 m^2/gm helped in the oxidation of cyclohexane, useful for various industrial applications [89]. Use of the surfactant – cetyltrimethylammonium (CTAB) in this case plays a vital role in producing such desirable physical feature. To study the effect of such ionic solution and surfactants on the synthesis of Fe_2O_3 nanoparticles, solution of iron pentacarbonyl and decane was sonicated separately in presence of 11-undecenoic acid, dodecyl sulfonic acid and octyl phosphonic acid [89]. The electrolytic solution formed an ionic bond at the surface of iron oxide nanoparticles that prevented them from agglomerating and produced fine,

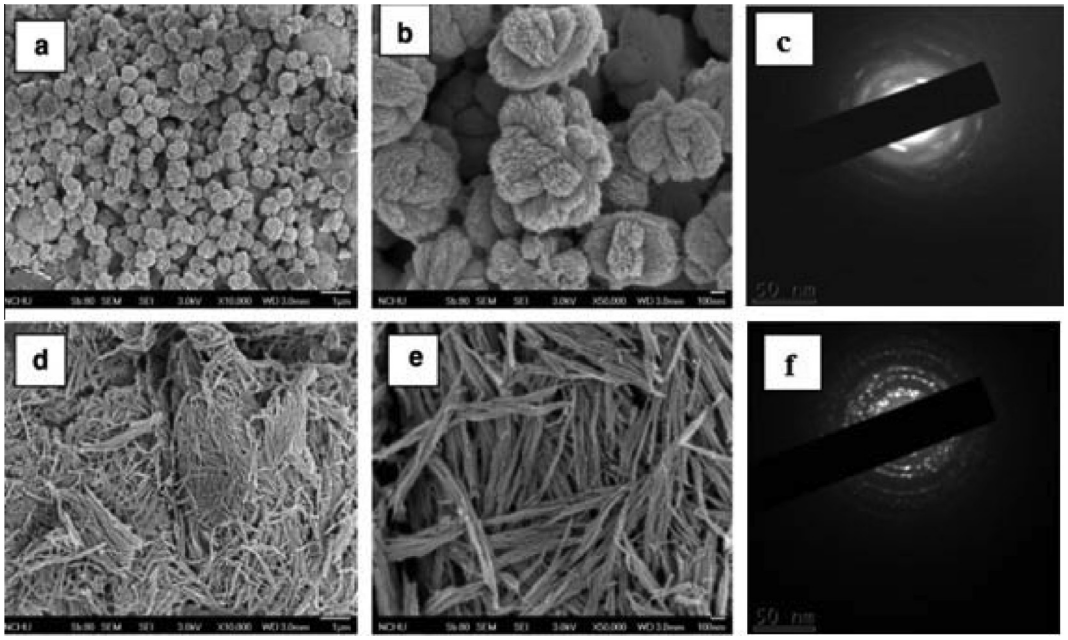

Fig. 7. CuO nanoparticles (top and bottom) synthesized using organic and inorganic reducing agent: (a–c) sample prepared using urea; (d–f) sample prepared using NaOH. Reprinted with permission from [88].

well-dispersed iron oxide nanoparticles [89]. The use of ionic solvents also helped in reducing the nanoparticle size and achieving higher yield. In an interesting case, sonochemically synthesized Fe_2O_3 nanoparticles formed a liquid core–shell structure comprising of a mixture of Fe_2O_3 nanoparticles (2–6 nm) and an ionic liquid 1-ethyl-3-methyl-imidazolium tetrafluoroborate encapsulated by polytetrafluoroethylene (PTFE) particles [140]. The Fe_2O_3 nanoparticles and 1-ethyl-3-methyl-imidazolium tetrafluoroborate slurry when dropped in PTFE powder, rolled due to surface tension to form such liquid filled spheres. This hydrophobic sphere, termed as magnetic marble, is shown in Fig. 8.

3.1.3. Metal Sulfide

Sulfur, a group VI oxygen counterpart, produces metal sulfides that feature similar catalytic properties as metal oxides. Among the diverse metal sulfide nanoparticles, molybdenum disulfide (MoS_2) is widely synthesized for its application in optics, electronics, catalysis etc. MoS_2 nanoparticles can be simply synthesized by sonicating $Mo(CO)_6$ and isodurene in presence of sulfur [20]. The sonochemically synthesized MoS_2 nanopowder showed prominent catalytic property. When compared against conventionally synthesized MoS_2 and commercially available catalysts such as: ReS_2 and RuS_2, for hydrodesulfurization of thiophene, sonochemical MoS_2 produced higher catalytic activity than the conventional sample, even better than the commercial and more-expensive catalysts [20]. Analyzing the sonochemical sample revealed spherical nanoparticles agglomerating to form clusters of ~15 nm in diameter as shown in Fig. 6. Compared to the conventionally synthesized sample, the sonochemical product, featured higher edge roughness, known to enhance the catalytic property of MoS_2. MoS_2 can also be synthesized in spherical form, similar to organic fullerenes [28,78]. Such MoS_2 nanospheres were synthesized via prolonged sonication of $Mo(CO)_6$, sulfur and o-xylene that transformed the initially formed MoS_2 nanoflakes into such structures [78]. In addition to MoS_2, sonochemically synthesized antimony trisulfide (stibnite Sb_2S_3) nanoparticles also show interesting changes with respect to sonication time [79]. Increasing the duration of sonication transformed the primary amorphous stibnite nanospheres to crystalline nanorods and nanowhiskers, which eventually formed only nanorods that crystallized along the (001) plane. Different morphology and changes have been reported during the synthesis of sulfide and similar chalcogen nanomaterials [141–144].

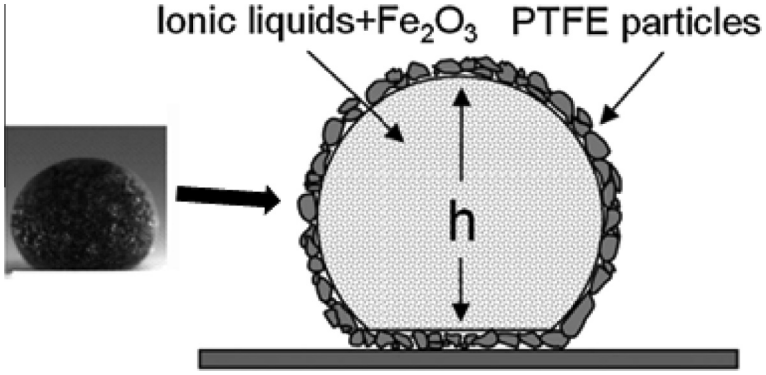

Fig. 8. Iron oxide based magnetic liquid marble, formed off a liquid core encapsulated by a hydrophobic layer. Reprinted with permission from [140].

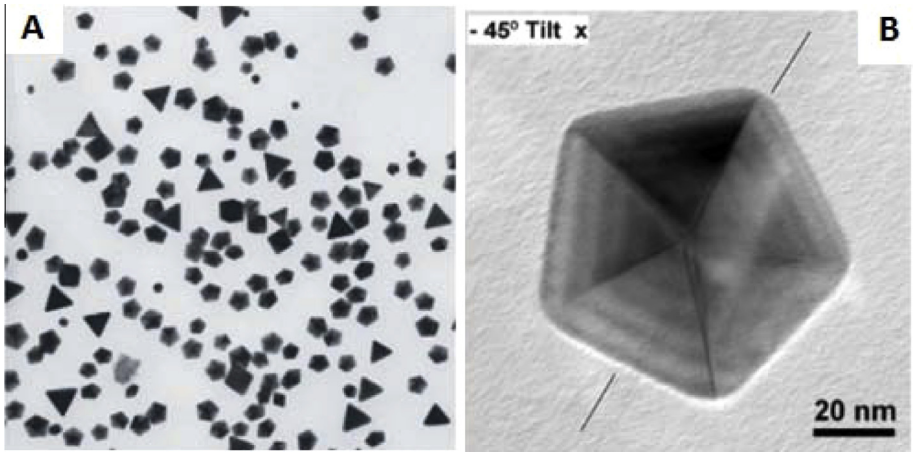

Fig. 9. (A) TEM image showing different shape of gold nanoparticles formed upon sonication of $HAuCl_4$. (B) TEM image of a pentagonal bipyramid gold nanoparticle at −45° tilt angle. Reprinted with permission from [147].

3.2. Metal

Transition metal nanoparticle in pure form is highly unstable and difficult to synthesize. Suslick's primary report on the sonochemical synthesis of amorphous iron was a ground breaking result that attracted a lot of interest towards sonochemistry – a milestone in this field [16]. Sonication of iron pentacarbonyl in decane at ice cold temperature produces pure, amorphous iron. The as-prepared sample when used for Fisher–Tropsch process and hydrogenolysis and dehydrogenation of saturated hydrocarbons showed higher catalytic activity than commercially available iron powder. Its high surface area, ~150 times higher than the commercial iron powder, was vital in enhancing the catalytic property. Even though the amorphous sample sintered to form crystals of ~50 nm upon heating, its catalytic property was essentially preserved. Amorphous nickel has been synthesized similarly from nickel tetracarbonyl and decane [17]. The as-prepared paramagnetic nickel showed good catalytic activity when dissolved in hydrogen peroxide: useful for electrochemical applications. Stabilizer, support etc. is otherwise required to synthesize stable metal nanoparticles. Iron colloids synthesized from $Fe(CO)_5$ in presence of oleic acid/PVP showed good stability and air resistance unlike their pyrophoric nano counterpart [145]. The as prepared amorphous, superparamagnetic iron colloids transformed to 3–8 nm crystals and grew in ferromagnetism with the application of heat.

Noble metals such as gold, platinum, silver, palladium etc. is easier to synthesize in sole form because of their natural stability [146–149]. Due to the extreme scaling, these metals, however, lack their normal chemical inertness in nanoform and offer applicable properties. Chloroauric acid ($HAuCl_4$), commonly used as precursor for the synthesis of gold nanoparticles, shows to produce gold nanoparticles in assorted shape and size upon sonication. These nanoparticles seen as prism, bipyramid etc. in Fig. 9(A), were synthesized sonochemically from an aqueous solution of $HAuCl_4$ and DMF in the presence of pre-synthesized gold nanoparticles (used as seed) and a stabilizing agent [147]. The role of stabilizing agent is quite crucial in the synthesis of noble nanoparticles as it helps to check their rapid growth rate. Varying input ultrasound frequency can also affect the growth rate of $HAuCl_4$ based gold nanoparticles [51]. Without the need of seed particles, Liu et al. report a facile way to synthesize gold nanocluster (AuNC) via sonicating $HAuCl_4$ in the presence of an organic protein – Bovine Serum Albumin (BSA) – used as a stabilizer [148]. The formation of these fine, stable and fluorescent AuNCs (~2 nm in size) was conspicuous from the changing color of the solution during sonication. Compared to AuNC prepared via solution phase method, the fluorescence emission of AuNC synthesized sonochemically shifted more towards the infrared region; likely due to their drastic size reduction. The red fluorescence of AuNC was completely quenched by copper (II) ion, while other ions such as Fe^{3+}, Ni^{2+}, Co^{2+}, Zn^{2+} etc. left the solution color unchanged rendering a copper (II) ion sensing application. Sonochemical synthesis of fluorescent AgNC from an aqueous solution of silver nitrate ($AgNO_3$) and PMAA (used as a capping agent) has also been reported [149]. The AgNCs formed sonochemically were stable and well-dispersed and showed tunable optical property. AgNC can be also be simply synthesized by replacing $HAuCl_4$ with $AgNO_3$ in the form of Au@AgNC in the previous report [148]. The silver ion liberated from the dissociation of $AgNO_3$ interacted with the already-formed gold clusters to produce Au–Ag nanocomposites. Gold–palladium (Au–Pd) nanocomposites can be similarly synthesized via sonication of sodium tetrachloroaurate ($NaAuCl_4{\cdot}2H_2O$), sodium tetrachloropalladate ($PdCl_2{\cdot}2NaCl{\cdot}3H_2O$) and aqueous sodium dodecyl sulfate (SDS) [62]. The formation of Au–Pd nanoparticle, like in [148], can be determined by observing the change in color of solution during sonication. The absorption spectra depict subsequent formation of each nanoparticle, with gold nanoparticles being first to form. The synthesized product analyzed using TEM and XRD showed fine deposition of palladium on the surface of gold nanoparticles, and formation of traces of carbon. Thickness of Pd coating and size of the Au core was understood to depend on their precursor concentration. The Au–Pd nanocomposite showed good catalytic potential when used for dehydrogenation of 4-pentenoic acid, which was higher than the total dehydrogenation done by Au and Pd individually [44]. Other noble metals such as: palladium [150], platinum [151,152], platinum-ruthenium [153] etc. have also been synthesized sonochemically for their catalytic applications.

3.3. Metal and Metal Compound with Support

To aid sonochemical processing, micrometer spheres have been widely used as support/template [28,130,134,154–156]. Microspheres of silica are commonly used for such role as it offers a benign and adhesive surface for material growth, and can be removed simply through etching. The added controllability coupled with the improved dispersion that comes with the use of microspheres has shown to improve catalytic property of active nanomaterials such as Fe, Ni, Mo etc. [19,28]. As demonstrated by silica-supported Fe and MoS_2 nanoparticles synthesized sonochemically, catalytic property of the sonochemical sample was much higher than the ones synthesized conventionally [19,28]. When tested for hydrogenation of CO (Fisher–Tropsch

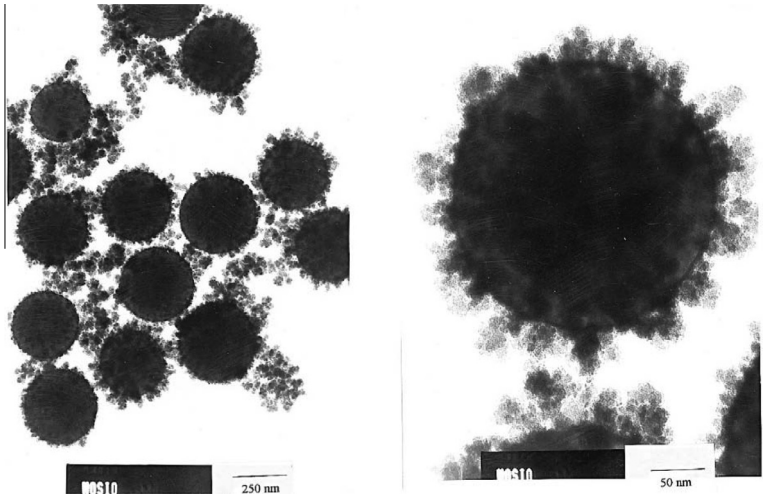

Fig. 10. TEM images, at different magnification, of molybdenum oxide nanoparticles synthesized over silica microspheres. Reprinted with permission from [156].

reaction), the sonochemical iron-silica product showed ten times higher catalytic activity than iron-silica powder prepared via incipient-wetness method [19]. Even at temperature below 250 °C, the sonochemical sample worked actively towards CO hydrogenation, while the conventional sample showed no activity. Similarly, MoS_2-silica nanocomposite displayed high catalytic activity towards hydrodesulfurization (HDS) of thiophene over a wide range of temperature [28]. Washing the MoS_2-silica with HF removed the silica core to form a hollow MoS_2 nanosphere. The excellent HDS of thiopene shown by such hollow MoS_2 was highly eminent and unmatchable for commercial and conventional MoS_2 nanoparticles. In addition to contributing to such improvements, sonochemical synthesis of MoS2 was simple, efficient and fast – completes in a single step. Furthermore, following a model for one growth and deposition, the process can be easily improvised to achieve different results. As reported, Mo_2O_5 nanoparticles were synthesized and successively coated over silica in a single step by sonicating a slurry of $Mo(CO)_6$, decane and silica microspheres [155]. Sonicating similar mixture under Ar, instead of air, produces Mo_2C nanoparticles instead of Mo_2O_5 that successively coat the silica microspheres [155]. Both Mo_2O_5 and Mo_2C nanoparticles (5–10 nm) were amorphous and porous in nature, but Mo_2O_5 nanoparticles, as seen in Fig. 10, showed better dispersion and coating over silica with coating as thick as 20 nm. Changing the solvent from decane to isodurene, $Mo(CO)_6$ produces a more stable version of molybdenum oxide – MoO_3, which in presence of sulfur produces MoS_2 nanoparticles instead of MoO_3, both of which subsequently coat the silica microspheres [28]. Alumina microspheres can also function as a viable support, especially in case of metals such as nickel that do not grow uniformly over silica [156]. Alumina offers a conducive surface and facilitates a uniform growth/deposition of nickel nanoparticles, which otherwise agglomerate and adhere poorly. Nickel nanoparicles grown on top of alumina forms a surficial bond that builds with temperature as seen in Fig. 11 [130]. The amorphous nickel in 11(a) upon heating subsequently crystallizes and reacts with the alumina surface to form $NiAl_2O_4$ as illustrated by Fig. 11(f). Therefore, following the basic guideline, new and different type of core-shell nanostructure can be simply synthesized in a collective sonochemical cycle.

3.4. Bimetal Alloy

Sonochemistry offers a facile way to synthesize metal alloy nanoparticles. Inferring from the growth of metal and metal compounds from the decomposing precursor, adding two or more metal precursor such as ‘iron acetate and copper acetate’ or ‘iron carbonyl and nickel carbonyl’ or ‘iron acetate and nickel carbonyl’ should form an alloy of respective metals upon sonication. Shafi et al. report on the synthesis of iron-nickel alloy - $NiFe_2O_4$, via sonication of iron carbonyl and nickel carbonyl [157]. Participation of each metal in the alloy formation process depends primarily on the vapor pressure i.e. volatility of its precursor, which significantly determines the proportion of each in the alloy. As vapor pressure of nickel carbonyl is higher than iron carbonyl, sonicating nickel carbonyl and iron carbonyl yields more nickel [90,92]. Quantity of nickel in $NiFe_2O_4$ was higher as expected, and therefore the amount of iron carbonyl had to be increased in order to obtain a proportional amount of both metals [157]. Both metal oxide, in nanoscale, being superparamagnetic, the as-prepared nanocomposite was similarly superparamagnetic, which after heating became ferrimagnetic and changed its state from amorphous to crystalline. Shafi et al. subsequently reported on the synthesis of iron-cobalt oxide nanoparticle following a similar approach. Cobalt tricarbonyl nitrosyl ($Co(CO)_3NO$) used alongside iron acetate produced amorphous and superparamagnetic $CoFe_2O_4$ nanoparticles with high surface area [158]. The as-synthesized product featured an average size of less than 10 nm and surface area of 176 m^2/gm. These sonochemically prepared ferrimagnetic nanocomposites display thin hysteresis loop signifying low loss and easy magnetization-demagnetization. Such unique magnetic field response, given the control to customize the quantity of each metal in the sonochemically synthesized alloy, is a coveted feature useful for various magnetic applications [159–161].

3.5. Zinc and Titanium

For their vast property and applicability, a separate section for the sonochemistry-based discussion of zinc and titanium is deemed important. ZnO exhibit the largest variety of structures and is one of the most promising and researched material [93]. From 1D and 2D materials such as dots, flakes, rods, flowers etc. to 3D spheres, hierarchical and hetero structures, ZnO can be synthesized in various morphology simply with a slight tweak, like a change of substrate, precursor, solution concentration, sonication time etc. in give rise to a different shape [21,52,162]. It can also be synthesized in conjunction with a different compound to form nanocomplexes using sonochemistry [45,141]. Like its morphology, application of ZnO nanomaterials is equally extensive; and is

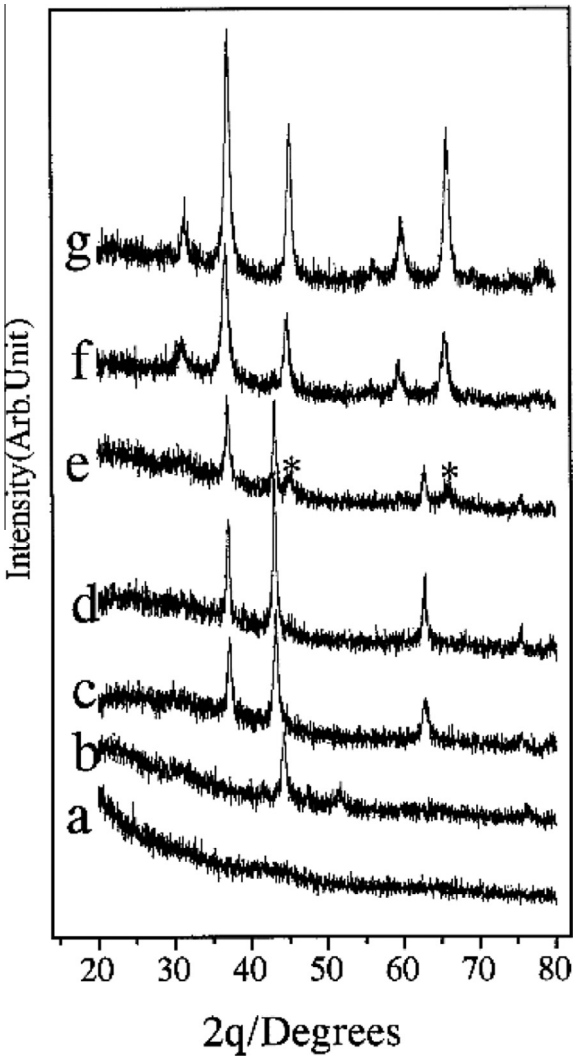

Fig. 11. Change in XRD pattern of Ni nanoparticles deposited on alumina upon annealing (a) as-synthesized amorphous nickel (b) crystallizes upon heating at 400 °C in Ar (c) and (d) forms NiO upon heating at 500 °C and 700 °C respectively in air for 4 h (e) forms $NiAl_2O_4$ and NiO upon heating at 800 °C (f) distinct peak of $NiAl_2O_4$ upon heating at 1000 °C (g) $NiAl_2O_4$ prepared separately for reference. Reprinted with permission from [156].

being used in making sensors, FETs, photo anodes, nanocantilevers, resonators, PZTs, purifiers, antibacterial bandages, sunscreens and many such practical applications [21,42,93,163]. Virtue of their small size, high surface area and purity imparted by sonochemical processing, use of such ZnO nanomaterials help improve the performance of such appliances and systems compared to the use of conventionally synthesized ZnO nanomaterials.

Zinc acetate dihydrate (ZAD) and zinc nitrate hexahydrate (ZNH) are commonly used precursors for sonochemical synthesis of ZnO nanoparticles. Both are ionic compounds and form crystalline ZnO nanomaterials when sonicated. In order to enhance the synthesis process, hexamethylenetetramine (HMT) is used alongside ZAD and ZNH that readily yields the hydroxyl ion necessary for ZnO synthesis. Our group members have synthesized various 2D and 3D ZnO nanostructure on different substrates using ZAD, ZNH and HMT [21]. The synthesis process is based on growth from and involves two steps: (1) Formation of seed layer via sonication of ZAD and isopropanol (2) Growth of ZnO on top of the seed layer via sonication of ZNH and HMT. ZAD and isopropanol is stirred vigorously to form a homogeneous solution and then sonicated to form a seed layer on a substrate. The seeded substrate is then immersed into an aqueous solution of ZNH and HMT, and sonicated under desired power and time. Depending on the concentration, time of sonication and choice of substrate, various forms of ZnO was obtained (as shown in Fig. 3 and 4). Utilizing the influence of such input parameters, 2D ZnO nanorods and 3D ZnO nanoflakes were grown with optimal features for making cortisol immunosensors [37]. This Anti-C_{ab} based portable sensor showed better detection towards cortisol than conventional and more expensive ELISA device. The chemical mechanism for ZnO formation basically involves reduction of ZNH to produce zinc ion that reacts with the hydroxide ion produced by HMT to form ZnO as shown below [164].

$$C_6H_{12}N_4 + 6H_2O \longrightarrow 4NH_3 + 6HCHO$$

$$NH_3 + H_2O \longrightarrow NH_4^+ + OH^-$$

$$Zn(NO)_3 \cdot 6H_2O \longrightarrow Zn^{2+} + 2NO^{3-}$$

$$Zn^{2+} + 2(OH)^- \longrightarrow Zn(OH)_2$$

$$Zn(OH)_2 - \longrightarrow ZnO + H_2O$$

ZnO nanowires synthesized accordingly on glass have shown to exhibit good UV and oxygen sensing property [111]. The effect of multiple cycle growth increased the nanowire density and decreased UV transmission – useful for sunscreen applications. The effect of concentration of ZNH and HMT has also been reported, as it induces explicit changes on the structure of ZnO [52]. Nanorods, nanocups, nanoflowers, nanodisks and nanospheres were produced specifically at specific concentration of ZNH and HMT, and with addition of certain chemical at calculated amount as shown in Fig. 12. The choice of solvent has also shown to influence the property of ZnO nanomaterial, not only shape but also its photocatalytic property [163]. Zinc acetate when added to an aqueous solution of methanol, ethanol and isopropanol formed nanoflakes, nanodisks and nanorods respectively [163]. Rate of photocatalytic reduction of chromium in water under sunlight was found to be higher for ZnO-ethanol based sample i.e. ZnO nanodisks compared to others. The increase in photocatalysis was assigned to its morphology, as samples prepared from ethanol were disk-like and exhibited higher surface area compared to others. ZnO nanoparticles also show distinct change in its size and formation with respect to temperature and sonication power. Sonicating a solution of $ZnCl_2$ and KOH under increasing power and temperature, in the range of 298–343 K and 0–45 W respectively, reduced the size of ZnO nanoparticles, their agglomeration, and also reduced the size distribution [50]. Samples at 343 K and 45 W showed smallest particle size (70 nm in average), better dispersion and distribution compared to other samples.

In addition to ZnO, titanium dioxide (TiO_2) is equally renowned for its photocatalytic potential and is widely used in making dye based solar cell [165,166]. TiO_2 and other compounds of titanium also possess strong piezoelectric property that is popularly used in making many devices such as sensors, converters and transducers – the ultrasound probe used in most sonochemical apparatus is made out of titanium alloy. Compared to ZnO, TiO_2 offer higher stability when used in photocatalysis and dye-based photocells, and their ability to grow in mesoporous form further improves their catalytic and other applicable features [165]. However, synthesis of mesoporous TiO_2 nanomaterials via convenient methods is difficult – (a) highly toxic phosphorous is formed during the process that binds to the TiO_2 particles intrinsically, which requires exhaustive purification. (b) Phosphorous-free methods require prolonged processing time of up to 10 days [167–169]. Sonochemistry provides an expedited route to the synthesis of non-toxic,

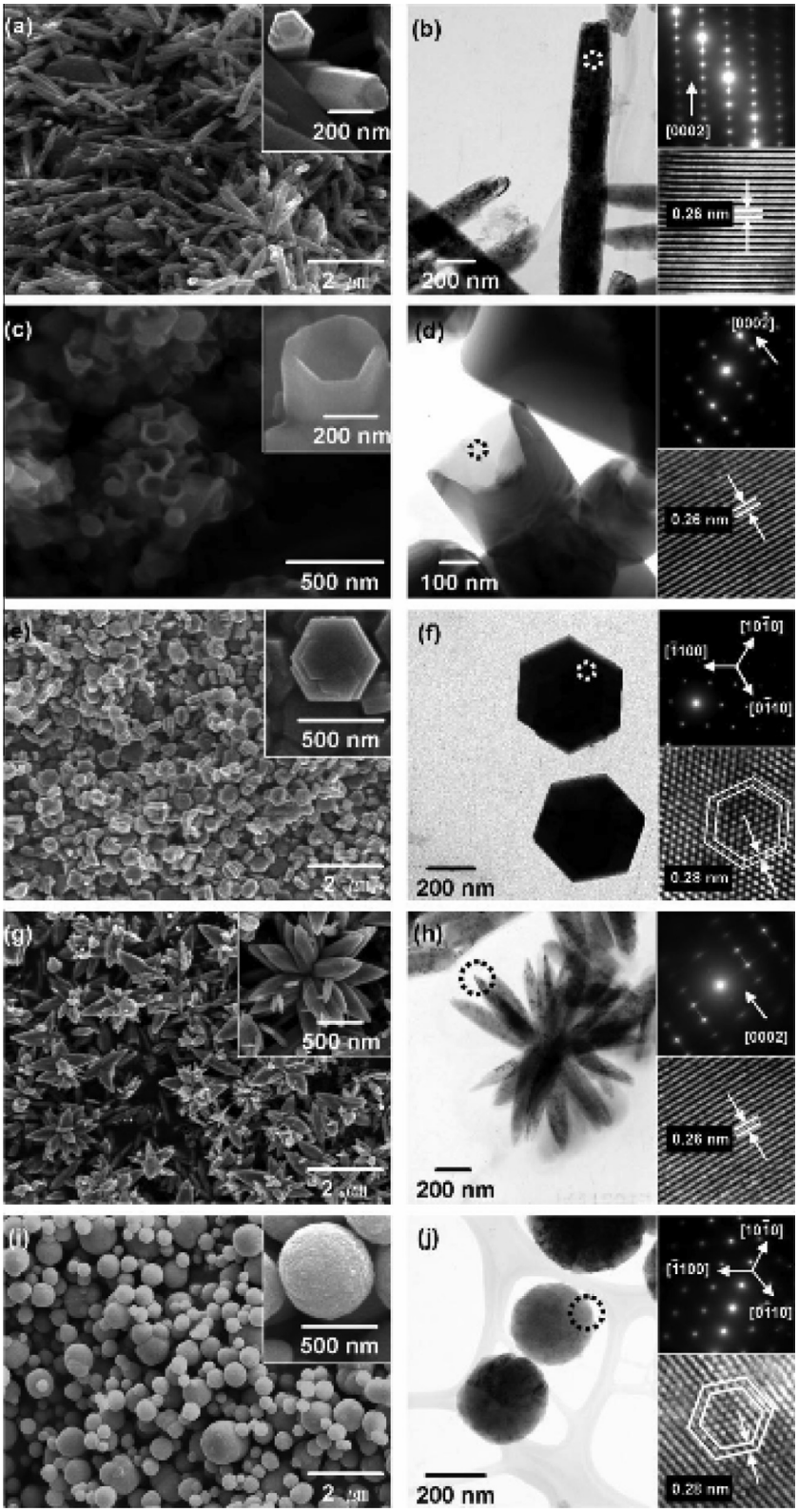

Fig. 12. Change in morphology of ZnO nanostructures caused by varying precursor concentration. Left shows SEM and right shows TEM image of ZnO nanorods, nanocups, nanodisks, nanoflowers and nanospheres in order from top to bottom. Reprinted with permission from [52].

amorphous, mesoporous TiO_2 nanoparticles featuring high surface area with the use of organic amines: decylamine, dodecylamine and octadecylamines [167,168]. Compared to the warmhole-like framework obtained with the use of amines, Yu et al. report on synthesis of TiO_2 nanoparticles with bicrystalline framework – anatase and brookite [168]. These sonochemically synthesized TiO_2 nanoparticles showed higher photocatalytic activity during degradation of pentane compared to commercially available P25.

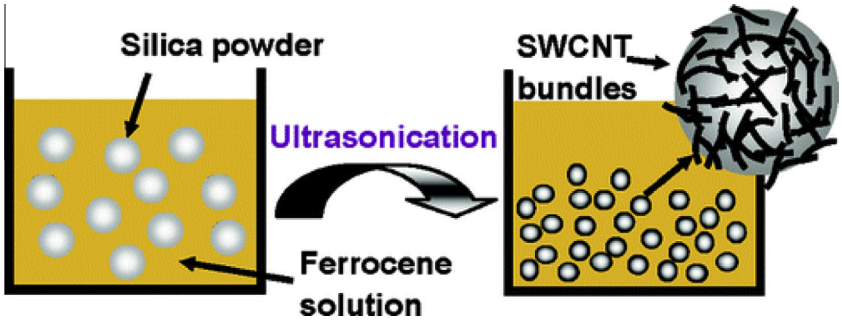

Fig. 13. Formation of single walled carbon nanotube on silica surface produced by sonication of silica spheres, paraxylene and ferrocene. Reprinted with permission from [171].

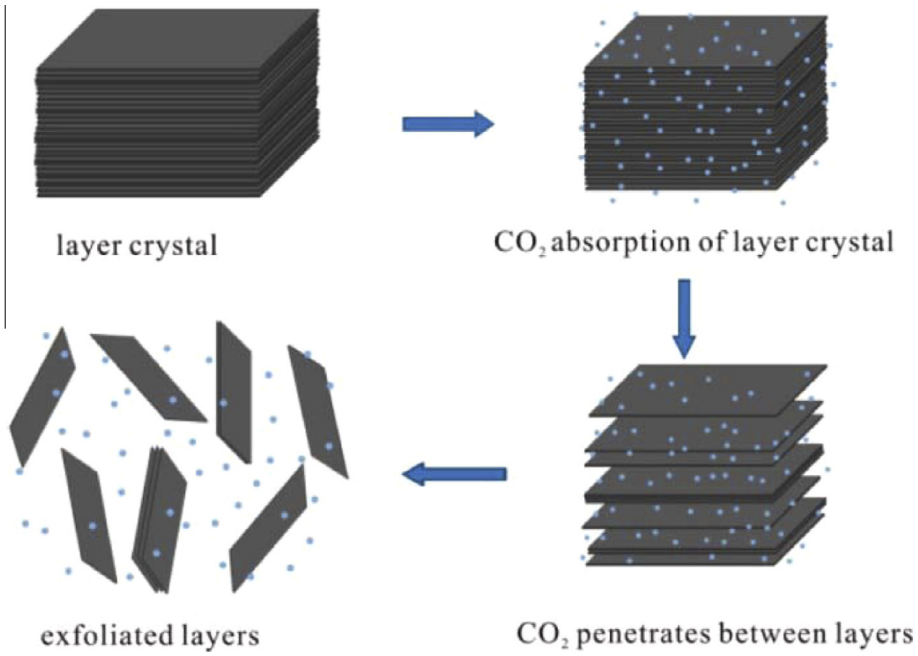

Fig. 14. Exfoliation of layered materials using supercritical CO_2 and ultrasound. Reprinted with permission from [84].

Such improved catalytic property was attributed to the high porosity and surface area of the sonochemical sample, which improved when synthesized in presence of triblock copolymer.

3.6. Carbon and Carbon Analog

While discussing the physical effect of ultrasound, we briefly referred to the synthesis of 2D MoS_2, BN, graphene, carbon nanotubes and other carbon related nanomaterials from their layered counterparts. Synthesis of such materials is greatly helped by the exfoliation effect of ultrasound that obviates the need of strict processing condition required by many conventional methods. To start, let us begin with the one widely known as the 'magic material' – graphene. Graphene synthesized through conventional means require high temperature, pressure and other stringent conditions that causes surface damages, modifications of chemical and physical characteristics, hybridization etc. While inability to process graphene down to few layers continues to challenge many physical methods, formation of graphene oxide that hinder graphene's conductivity remain a major concern for most chemical based methods. Exfoliation of graphite under ambient condition to produce few layered graphene with the use of power ultrasound has proved to be easy and facile. Xu et al. demonstrate how few layered graphene sheets can be obtained in a short and simple way via sonication of graphite flakes in styrene (used as a solvent as well as stabilizer) [26]. In this experiment, graphene sheets produced from exfoliation were successively functionalized by polystyrene (that formed from polymerization of styrene during the process). Polystyrene stabilizes the exfoliated graphene sheets and prevents them from agglomeration, multiple layer formation and folding. Although it roughened the graphene surface and modified the sp^2 hybridization, the process did not oxidize the functionalized graphene and produced few layer standing graphene sheets – 80% of the sample composed of 5 or less layers. Similarly Lotya et al. report on exfoliation, dispersion and successive deposition of graphene in a substrate via sonication of graphite in presence of a surfactant – sodium dodecylbenzene sulfonate [29]. The exfoliated graphene flakes consisted of mostly 5 or less layers while ~3% of them were monolayer graphene, and essentially showed no significant defect on its basal plane. In a very similar way, carbon nanoscrolls, a material similar to multi walled carbon nanotubes (MWCNT), has been obtained from graphite. 2D graphite sheets exfoliated from ultrasonication and with the help of an exfoliating agent – potassium metal compound (KC_8), fold to

form carbon nanoscrolls upon sonication [12]. As reported, graphite left for sonication for 6 h in absence of KC_8 showed formation of graphite plates with modest scrolling, while the ones exfoliated only with KC_8 showed negligible nanoscrolls. The use of ultrasound and the time of sonication was shown to be vital for the formation of carbon nanoscrolls. Synthesis of another material of carbon–carbon nanotubes, with which the grand design of making a space elevator now seems a viable proposition, has also been reported via sonochemistry [170,171]. In this two-step process, paraxylene (used as carbon source), ferrocene (used as catalyst) and silica spheres (used as support) was first sonicated, which within 20 min of sonication produced single walled carbon nanotubes (SWCNT) that subsequently adhered to the silica sphere surface as shown in Fig. 13 [171]. Secondly, the sonicated solution was washed with HF to remove the silica particles to produce a fiber-like structure consisting mostly of SWCNT. The use of silica powder was vital as samples sonicated without silica powders showed no SWCNT formation. Using sonochemistry, in just 2 steps and within an hour, highly pure SWCNT with nominal defects can be synthesized that do not require prolonged time, extreme processing condition or further purification like many other methods [172,173]. Replacing silica spheres with silica nanowires, Sun et al. report synthesis of hydrocarbon nanostructures such as hydrocarbon nanotubes, hydrocarbon nanoonions etc. via similar approach [174,175]. Higher interlayer spacing, of up to 59 nm, shown by these sonochemically prepared hydrocarbons can be thought for new applications.

Hexagonal boron nitride (h-BN) exhibit property similar to graphene and is also known as 'white graphene'. Sonochemical synthesis of h-BN, MoS_2 and WS_2 via ultrasonic exfoliation showed to produce single layered BN, MoS_2 and WS_2 sheets demonstrating consistent property with their bulk counterparts [84]. Supercritical CO_2 used as an exfoliating agent penetrated into the respective precursors to cause such exfoliation. The temperature of the solution did not exceed 45 °C, and no stabilizing agent was needed to uphold the exfoliated sheets. A schematic diagram of the exfoliation process is shown in Fig. 14. Sonochemistry obviates the need of high temperature and unnecessary chemicals and offers an appealing alternative to most conventional methods that are known to affect the dielectric property and chemical stability of such BN, MoS_2 and WS_2 2D nanomaterials [84].

3.7. Protein and Biological Compound

Ultrasonically synthesized biological materials such as protein microspheres have found widespread applications such as in drug delivery, biomedical imaging, tumor treatment etc. [31,39,40,125]. Protein microspheres are capsule-like structure with an albumin shell covering a non-aqueous liquid or gas. Their synthesis is essentially helped by the ultrasonic oxidation of cysteine to form disulfide cross-links that form the protein shell [31]. Unlike most covalent surface modification, Toublan and co. report on electrostatic layer-by-layer assembly of a vegetable oil filled protein microsphere synthesized from ultrasonication of bovine serum albumin (BSA) [39]. The surface of these microspheres was successively modified to attach them to the integrin receptor overly expressed by tumor cells. Replacing BSA with sodium polyglutamate (SPG), helped obtain these microspheres in submicron range [176]. The small size of such SPG shell microspheres can easily pass through leaky vasculature to target tumor more effectively. Protein microspheres synthesized from BSA and filled with fluorocarbon have been synthesized for their potential use in imaging as well. Compared to fluorine and other fluorine based agents, microspheres with fluorocarbon offer higher signal to noise ratio when used as magnetic resonance imaging agent as shown in Fig. 15 [40]. The high signal to noise ratio was attributed to the effective encapsulation from ultrasonication that helped to deliver the fluorocarbon (imaging agent) specifically to the target, with amount up to six times compared to conventional cases. In addition to fluorocarbons, wide range of potential imaging agents can be simply encapsulated with the use of ultrasound to achieve higher contrast and life time. The lifetime of these imaging agents can be improved by modifying the encapsulating shell as well, which can also help in reducing the size of such microspheres. In addition to the facile approach and indiscrimination towards agent selection, the other important feature of these sonochemically prepared microspheres is their innocuousness. Typical polymer based or chemically cross linked protein microspheres induce immune responses when subjected to the body, while sonochemically synthesized ones do not trigger any immune changes [177].

In addition to material synthesis, ultrasound is also used for many common applications such as cleansing, imaging, catalysis, plating, drug delivery etc. [178–182]. It is popularly used in chemical reactions to expedite the reaction rate, thereby obviating the need of foreign chemicals or catalysts. The Nobel prized Heck reaction that require up to 72 h for the formation of sp^2 hybridized carbon bond was completed within 3 h with the use of ultrasound [183]. Moreover, ultrasound setups (including sonochemistry) are cost efficient and therefore can be accessed by large group of people including individual researchers and students. Various sonochemical apparatus such as ultrasound bath, ultrasound tank, immersible ultrasound horns, probes etc. capable of generating wide range of ultrasound frequency and power are readily available, which helps in the evolution of this field.

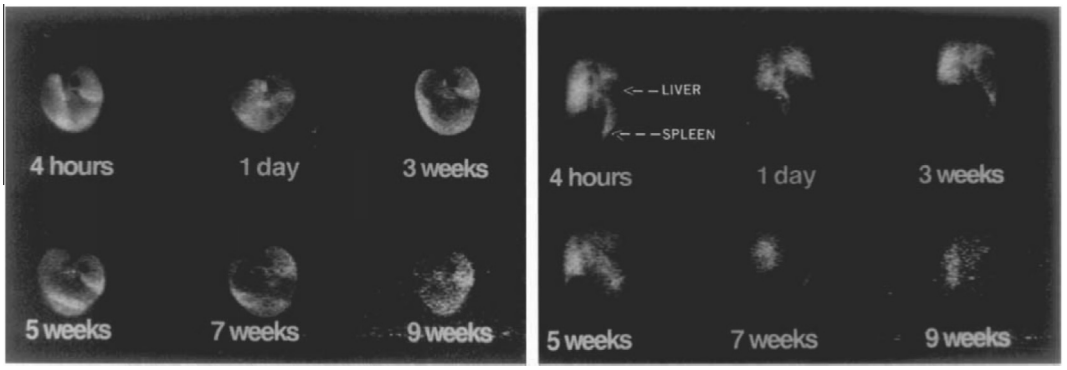

Fig. 15. MRI images of a rat after injection of microspheres. (a) Transverse images with respect to time of the liver. (b) Coronal images taken at the same time, shows accumulation of microspheres in the spleen. Reprinted with permission from [40].

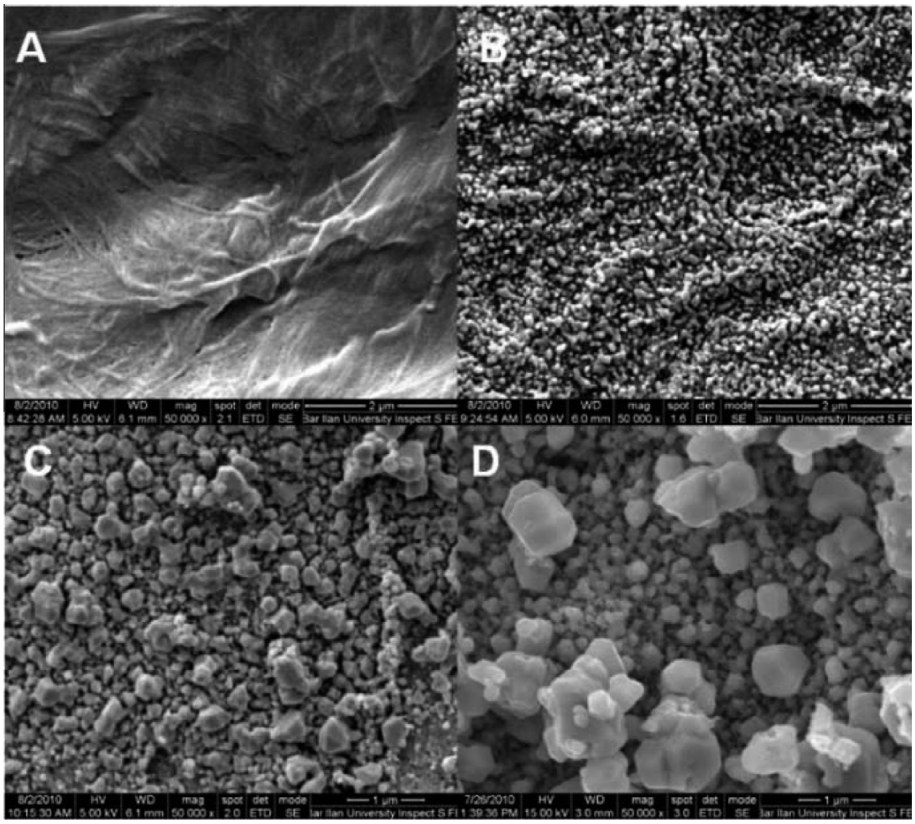

Fig. 16. SEM images of silver nanoparticles grown on paper with respect to time of sonication, at magnification 2 μm (A and B) and 1 μm (C and D). (A) Paper before sonication. (B) After 30 min of sonication. (C) After 60 min of sonication. (D) After 120 min of sonication. Reprinted with permission from [34].

4. Advancements and Engineering

In addition to assisting current technology, sonochemistry have facilitated numerous advancements and new applications such as: optical sensing, digital olfaction, environment remediation through nanomaterials, MRI through protein microspheres, graphene processing through ultrasound exfoliation etc. [18,116,43,148,177,184,185]. Similarly, a diverse group of chemical and biological materials have been synthesized sonochemically with ease [26,29,25,31,171]. In addition to improving existing technology, sonochemistry has unraveled new applications for making advanced devices and systems. The benign sonochemical approach enables the use of fabrics, and flexible and low melting point materials, allowing sonochemistry exclusive privilege to use them as substrate, template or support for nanomaterial growth [21,33,34]. From graphene to cotton and nylon, even papers have been used as substrates to grow nanomaterial on top. As a result, sonochemically synthesized nanomaterials have reached out to special cases in catalysis, sensing, solar energy harvesting etc. [44,80,42,163].

4.1. Substrate Versatilty

Use of flexible and low melting point substrate for nanomaterial growth can help boost modern electronics. Our group members have used PET, a polymer with melting point of 250 °C, as a substrate in addition to SiO_2/Graphene and Si/Graphene for sonochemical seed growth of various 2D and 3D ZnO nanostructures [21]. Depending on the type of substrate used, the morphology and physical property of ZnO nanomaterials changed prominently. In addition to growth, ultrasound can also be used to modify the chemically inert surface of various polymers such as polyvinyl chloride (PVC), polythene etc. to enable electronic printing [186]. Considering the manufacturing cost and prevalence of such polymer, this improvement can greatly minimize solid state fabrication cost in future. Kotlyar et al. report on silver nanoparticle growth and deposition on PMMA via sonication of PMMA chips and silver nitrate-ethanol solution [187]. The widespread use of PMMA in making windows, protective eyewear, optical fibers, windshields etc., along with the effective IR blocking characteristics of silver can help advance many commercial and scientific fields. Silver nanoparticles also feature useful antimicrobial properties that can used for different sanitary and medical based applications [188–191]. In addition to polymers, paper can also be used as a viable substrate to coat silver nanoparticles [34]. In a typical case, a parchment paper was immersed into an aqueous solution of $AgNO_3$, ethanol and ethylene glycol and sonicated under varying $AgNO_3$ concentration and sonication time. Samples were prepared at 25, 50 and 100 mM $AgNO_3$ concentration and 25, 30, 60 and 120 min sonication time, few of which are shown in Fig. 16. The stability and depth of coating of the 100 mM/120 min sample was higher, nevertheless, the antibacterial property was fairly the same in all case. In a single and simple step, silver coated papers showing effective antibacterial property for over 6 months can be prepared and potentially be used for food packaging, making napkins and tissue papers etc. Use of fabric can further advance these applications. Perkas et al. report the use of ultrasound to coat nylon with silver nanoparticles [192]. The silver coated nylon showed steady antibacterial property over time, and even after multiple washing. ZnO possess similar antibacterial property and is comparatively inexpensive than silver. The morphological diversity and useful physical property of ZnO nanoparticles, common availability of ZnO precursor, easiness in ZnO synthesis etc. has helped explore

uncommon materials and fabrics for such applications [33,193a,b]. In a typical case, Perelshtein el al. report in-situ synthesis of ZnO nanoparticles from zinc acetate and their subsequent seeding-growth onto cotton [33]. Compared to processes that require stabilizers and foreign chemicals, the contaminant-free sonochemical cotton showed consistent antibacterial property even with minimal ZnO coating because of the high adhesion [33,194]. Given the economical nature of the process, such fabric can not only be used in hospitals but also in general to prevent infections and diseases. The 'smart textile' concept can be simply revolutionized to uplift our health and living standard.

4.2. Sonofragmentation

In addition to materials synthesized from chemical reaction and exfoliation, ultrasound, during sonochemistry, can help process nanoparticles via physical collision. This application i.e. sonofragmentation, is derived from the entailing effect of cavitation that accelerate solid particles to strike and fragment [24,195]. Fragmentation is caused by particle colliding with: (a) other particles, (b) vessel wall or (c) the ultrasound probe or the vibrating effect of shockwave that couple elastically with suspended particles. To investigate their individual contribution, Zeiger et al. studied the effect of each process – particle-shockwave interaction and (a), (b), (c) by isolating the other three [24]. The effect of particle-horn collision and particle-vessel collision was found to be insignificant as well as the effect of increasing particle concentration, which produced no remarkable change in fragmentation yield. It was concluded that the effect of shockwave-particle interaction is major in inducing fragmentation considering the fact that increasing concentration, however, increases (1) Vander Waals' attraction (2) effect of screening, both of which hampers particle collision. Time of experiment, applied power and frequency, use of surfactants etc. can individually affect the overall process of fragmentation [83,185,196]. Low frequency and addition of surfactants shows to improve fragmentation yield, while increasing power and experiment time shows to reduce the size of fragments and produce a uniform size distribution. The ability to format the process with applied parameters helps in engineering a sonofragmentation system to overcome the limitations of conventional processes such as ball milling, grinding etc. Sonofragmentation has become a handy tool to prepare pure and sinterable alumina powders in the submicron range useful for common applications such as lamination. Highly pure alumina fragments with size less than 100 nm were processed via sonofragmentation that showed good sinterability which otherwise require high processing temperature

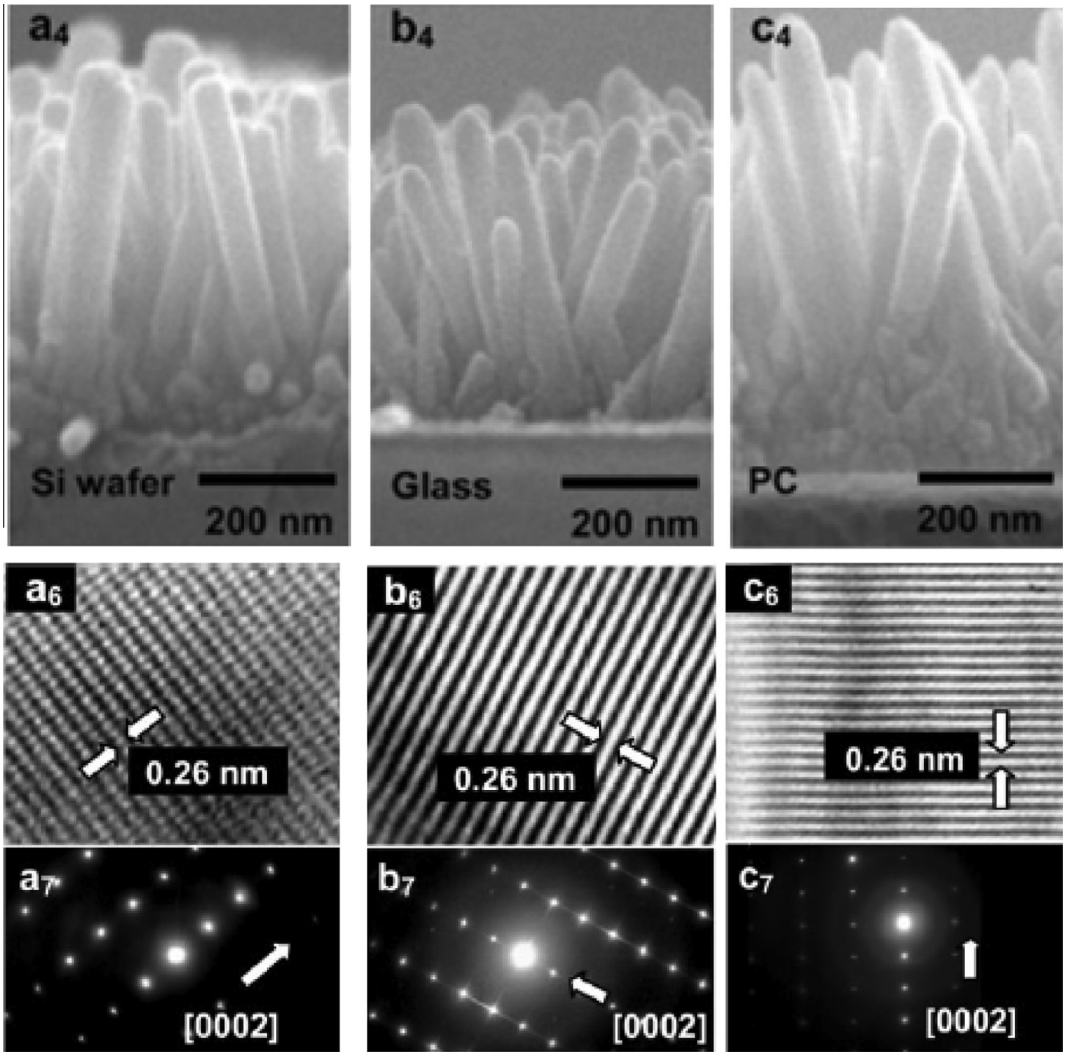

Fig. 17. Vertically aligned ZnO nanorods oriented in the [0002] crystal plane grown on top of: Si wafer (a_4, a_6, a_7), glass (b_4, b_6, b_7) and polycarbonate (c_4, c_6, c_7) respectively. Reprinted with permission from [199,130].

of up to 1700 °C or addition of sintering aids [185]. Sonofragmentation has also found its use in the commercial market – in processing talcum powder with better absorption [198]. Talc with low particle size and variance, low aggregation and high purity has been processed via sonofragmentation which otherwise require stabilizers, high power and multiple step post-processing [185,198].

4.3. Aligned growth and patterning

Aligned nanomaterial growth offers a low-loss, continuous transport channel that can help improve applications such as in sensing, antennas, photo cells etc. [199]. Commonly used methods such as vapor liquid solid, hydrothermal, self-assembly, e-beam lithography laser ablation etc. involve complicated means that can be simplified with the use of ultrasound [200,201]. Highly aligned ZnO nanorods, in the form of array, have been synthesized sonochemically on top of various substrates such as silicon wafer, zinc sheet, flexible polymer and transparent glass as shown in Fig. 17 [199]. The substrate, in each case, was coated with photoresist in a patterned way using UV lithography first and then sonicated. The sonicated substrate when washed with acetone, removed the photoresist and the ZnO on top to produce ZnO nanorods array. Following the same procedure, Jung *el al.* appeal using other substrates and nanomaterials.

Ultrasound can also be used to align or separate micro and nanoparticles depending on their compressibility [202]. Diamond nanoparticles (~5 nm) dispersed into a small rectangular tank filled with water, showed to align at the node of ultrasonic standing wave when sonicated with a high frequency piezoelectric plate transducer [202]. Such pattern depends primarily on the input frequency, as the distance between each alignment lines vary with changing frequency. The acoustic radiation force acting on the immersed particles depends on the property of the liquid and the particle basically, and is given by Eq. (7)

$$F = -\nabla\left(\frac{2}{3}\pi R^3\left[\frac{P^2}{\rho_m c_m^2} - \frac{P^2}{\rho_p c_p^2} - \frac{3\rho_m(\rho_p-\rho_m)}{2\rho_p+\rho_m}\vartheta^2\right]\right) \tag{7}$$

where R is the radius of the particle to be aligned and governs the radiation force felt by the particles i.e. microparticles are subjected to 10^9 times higher force compared to nanoparticles. P is the time averaged pressure inside the liquid due to ultrasound and can be derived from simple wave equation as shown in Eq. (8) Density of the medium and the particle are given as ρ_m and ρ_p respectively and speed of sound in the medium and the particle are c_m and c_p respectively. Similarly ϑ is the medium displacement velocity written as shown in Eq. (9). In Eqs. (8) and (9), P_{x0} and P_{y0} are the maximum pressure at x and y direction. Similarly k and ω represents the wave number and frequency.

$$P^2 = \left(\frac{P_{x0}^2 cos^2(k_x x) + P_{y0}^2 cos^2(k_y y)}{2} + P_{x0}P_{y0}\cos(k_x x) * \cos(k_y y) * \cos[(\omega_y - \omega_x)t]\right) \tag{8}$$

$$\vartheta^2 = \frac{1}{2\rho_m}\left[\frac{k_x^2 P_{x0}^2 sin^2(k_x x)}{\omega_x^2} + \frac{k_y^2 P_{y0}^2 sin^2(k_y y)}{\omega_y^2}\right] \tag{9}$$

4.4. Sensor

The sensor industry has been helped by nanotechnology like no other. New and portable sensing technology have flourished with the evolution of nanomaterial and virtuously challenged conventional sensing methods. In case of most biomedical and gas sensors, the sensing efficacy is mainly determined by the amount of immobilized enzyme or chemical that react with the chemical to be sensed. With their high surface to volume ratio, nanomaterials enhance absorption that can help immobilize enzyme more effectively and provide higher reaction sites than bulk materials. Monodispersed and amorphous nature of most sonochemically synthesized material can further enhance the immobilization and reaction process and eventually sensing [152,81]. Sensors as small as the size of a thumb showing excellent sensitivity, selectivity, detection limit and range, and that which do not require special temperature and physical condition have been fabricated with the help of ultrasound [203]. One such case is the sensing of ethanol where sonochemically fabricated ZnO nanorods based gas sensor obviate the need of high sensing temperature and produce fast and consistent results at 140 °C [203]. Whereas most solid state sensors, even ZnO nanostructure based gas sensors fabricated from other methods, demand temperature of above 300 °C or need of surface catalyst for ideal sensing. Comparing with other ZnO counterparts for ethanol sensing at 200 ppm concentration, the sonochemical version showed sensitivity (S) of 224.2 against 47 and 25.2; S of ~25.2 (20.5 actual) was produced at just 10 ppm concentration. The improved sensitivity and detection at low temperature was ascribed mainly to the fine nanoparticle size and distribution due to sonochemistry.

For their widespread applications in food processing, environment monitoring, medical diagnosis etc., glucose sensors are the most common devices in the sensing field [204]. Monitoring glucose level in blood can help prevent obesity, diabetes and various other health conditions. To cope with the growing need, various sonochemically processed enzyme and non-enzyme based glucose sensors have been reported that show better sensitivity and features [204,86,205,81]. In one case, microelectrode arrays based glucose sensor promising 'unrivalled sensitivity' has been devised in a very interesting fashion [86,205]. With respect to single electrode, microelectrode array fabrication, though expensive, can greatly improve detection limit and sensitivity, and can also be used to sense more than one chemical. Polydiaminobenzene coated gold substrate was sonicated to form cavities that structured the formation of microelectrode arrays, in a very economical and elegant manner. This microelectrode sensor can supposedly be used to sense glucose, ethanol, oxalate, pesticides and other chemicals. Another glucose sensor based on sonochemically grown PAMAM-Au nanocomposite have been reported demonstrating the significance of sonochemical processing [204]. As revealed by TEM, sonochemically prepared PAMAM-Au samples were smaller and well-dispersed compared to the ones grown via stirring, which helped in improving sensing. Additionally, the increase in electrical conductivity of PAMAM due to the inclusion of gold nanoparticles was also significant, and the sensitivity, detection limit and response time shown by this device was better than the ones previously reported. Therefore, for the biocompatible nature of gold and good selectivity shown by the sensor towards glucose in presence of other chemicals like uric acid, cysteine, glutamate etc., the author deem this sensor to be clinically usable.

Biomedical sensors are mostly based on enzymatic reaction i.e. substances such as hemoglobin, glucose oxidase etc. are immobilized to react and sense a specific chemical. These sensors offer good sensitivity and responsivity but limited use and lifetime because of enzyme instability and degradation [81]. As in previous case [204,86,205], the microelectrode array and PAMAM-Au nanoparticles serve to immobilize the enzyme – glucose oxidase (GOD) and react with the glucose sample. With the advancement in nanomaterial processing, different catalytic metals and their alloy have been synthesized and explored as enzyme alternatives. Platinum and its alloy, for their high catalytic property, have shown good potential [80,81]. Sonochemically synthesized PtM nanoparticle alloy (where

M = Au, Pd or Ru) has been used to replace GOD in making non-enzymatic glucose sensor by modifying a glassy carbon electrode (GCE) using ultrasonic-electrochemical deposition [78]. Since the catalytic behavior of PtM depends not only on metal 'M' but also on the surface where it is deposited, facile and controlled modification of GCE surface with materials offering high surface area such as graphene, chitosan, MWCNT etc. can help its electrocatalytic performance. Xiao et al. understood that surface modification of GCE with MWCNT and an ionic liquid (IL) – trihexyltetradecylphosphonium bis(trifuoromethylsulfonyl)imide, provides better support to the platinum alloy nanoparticles and work synergistically to improve sensing compared to bare GCE and MWCNT/GCE. Assessing the composite electrode with various combinations of alloy and surface modification, the PtRu-MWCNT-IL/GCE electrode showed best sensitivity towards glucose. Xiao et al. also report on non-enzymatic H_2O_2 sensing based on PtAu nanoparticles deposited separately on GCE and indium tin oxide (ITO) surface, modified with chitosan (Ch) – IL via ultrasonication [80]. The sensitivity improved when Pt and Au were mixed in the ratio of 1:3 and also increased gradually from Pt_1Au_3/GCE to Pt_1Au_3-Ch/GCE and peaked with Pt_1Au_3-Ch-IL/GCE showing very low detection limit of 0.3 nM. In both cases [80,81], stability, susceptibility and repeatability shown by each sensor was excellent. A non-enzymatic dual gas sensor based on sonochemically synthesized SnO_2 quantum dots has also been reported, that could detect CO under 300 °C and CH_4 over 300 °C [206]. Comparing against a similar sol–gel based SnO_2 gas sensor, for detection of CO at 1000 ppm concentration, sensitivity of the sonochemically derived one was 147 – nearly 3 times that of the sol–gel version. Such high response was mainly attributed to the large surface area of sonochemically synthesized SnO_2 quantum dots that helped in gas absorption – 257 m^2/g compared to 80 m^2/g of sol–gel.

In addition to quality growth, the feature that makes sonochemistry pertinent to sensor and similar devices is its ability to perform on-chip synthesis over a wide range of substrate. As an alternative to on-chip synthesis, a buffer mixture comprising of uniformly distributed nanoparticles in a selected chemical can be prepared ultrasonically and deposited over a substrate. With this option, nanoparticles can be deposited over desired substrates that lack a good surface for growth. Physical methods such as vapor liquid solid, vapor deposition, laser ablation etc. process under high heat that can damage the biosensor chip and therefore cannot facilitate on-ship synthesis. This impose the need to grow nanoparticles in a different material and then transfer them to the sensor chip. The main challenge now becomes not only to transfer these nanoparticles without damaging but also to prevent them from clustering, as clustering reduces the active area and hamper their sensitivity. Sonochemistry simply obviates this concern. As discussed previously [80,81], sensitivity was improved by the large surface area rendered by ultrasonic agitation of Ch-IL and MWCNT-IL that facilitated uniform dispersion of nanoparticles. Hence, ultrasound not only plays a crucial role in obtaining fine, unagglomerated nanoparticles but also in preparing a conducive surface. Compared to CNTs and Chitosan, graphene offers a higher surface area, and can be used as a support to deposit nanoparticles into sensors' electrode [95]. In situ synthesis of Fe_3O_4 nanoparticles and its successive integration into reduced graphene oxide (RGO) using ultrasound, when deposited into GCE has shown to produce a competitive H_2O_2 sensor without the use of any ionic liquids [95]. This biosensor when further modified with hemoglobin (Hb) – Fe_3O_4/RGO/Hb-RGO produce excellent sensing results. Compared to nanocomposite sample synthesized from different methods such as, microwave heating, hydrogen reduction, conjugation chemistry, controlled assembly etc., sonically synthesized Fe_3O_4 nanoparticles were far more refined and evenly dispersed into RGO that lends to sensing.

Sensors reviewed so far were enzyme or non-enzyme based that relied on the electrochemical reaction between the enzyme/non-enzyme and the chemical. Based on the reaction, sensing is reported in the form of a signal and evaluated in terms of detection limit, response time, SNR value etc., which is hampered by electrical interference and loss. How easier would it be if one can determine the presence of a certain chemical merely by visualization! Optical sensors offer such convenience. These sensors produce/change color in response to certain chemical. Sonochemically synthesized fluorescent nanoparticles have been used widely to make optical sensors [148,43]. Among them, silver and gold nanoparticles are the ones popularly used because of their intense fluorescence, biocompatibility and low toxicity [148,207]. However, control over their growth is difficult, as these nanoparticles quickly form large structure and require a growth inhibiting chemical; as a result the synthesis process can take up to 3 days [149]. Stabilized fluorescent gold nanoclusters (AuNCs) have been sonochemically synthesized from $HAuCl_4$ in an expedited fashion [148]. The sonochemically synthesized AuNCs showed excellent sensitivity and selectivity towards copper (II) ion – a 50 μM of Cu^{2+} solution completely quenched the red fluorescence of AuNC while other ions such as Fe^{3+}, Ni^{2+}, Co^{2+}, Zn^{2+} etc. left the solution color unchanged. Compared to AuNC prepared via phase solution method, the fluorescence emission of this sample shifted more towards the infrared region. This signifies that sonochemically synthesized AuNCs have low tissue absorption and can be better used for biological applications. On replacing $HAuCl_4$ with $AgNO_3$, gold–silver alloy nanoclusters (Au–AgNCs) were obtained that sported yellow fluorescence and good sensitivity towards Cu^{2+} as well. Ag nanoclusters from $AgNO_3$ and polymethylacrylic acid (PMAA) – used as a stabilizer that also prevents AgNCs from oxidation, has also been separately synthesized via sonochemistry, and can be useful in biological and chemical optical sensing [149]. In addition to noble metals, sonochemically synthesized carbon and zinc based nanomaterials also possess good fluorescent properties [43,45]. SWCNT stabilized with double stranded DNA (dsDNA) can function as a dual optical sensor for H_2O_2 and glucose [43]. A unique feature of these sonochemically synthesized fluorophores is their reversibility, which allows repeated use of the same sensing solution. The bright red fluorescence flashed by the SWCNT-dsDNA was diminished upon addition of H_2O_2 and glucose. The zinc nanorods based protein sensor reported by Pan et al. however works in the opposite way [45]. Contrary to standard decrement, different proteins like human serum albumin (HSA), BSA, bovine hemoglobin and egg albumin, when reacted with Zinc (II) – bis(8-hydroxyquinoline) nanorods increased their photoluminescence as an illustration of sensing. These sonochemically synthesized fluorescent particles continue to offer new features and functions to make optical sensing more interesting and advanced.

4.5. Photovoltaic

The immense advantage of harvesting solar energy has led to proliferation of different types of photovoltaic cell. Many of them such as thin film, dye-sensitized, quantum dot, printable solar cell etc. have benefitted with the use of nanomaterial. Photo active nanomaterials when used in making solar cell electrodes, naturally improve photochemical reaction due to their high surface area. In addition to the advantage from their nanophysics, such improvement can also be induced via structural variance i.e. synthesizing hetero and hierarchical structures using sonochemistry. Hierarchical nanostructures made from two or more nanostructures helps to abridge interparticle separation and smoothen electron channeling [42]. Sonochemically synthesized SnO_2 and ZnO hierarchical structures used in making dye-sensitized solar cells (DSSC) have shown to produce an efficiency of 6.40% (compared to 5.21% with SnO_2

nanoparticles) and 6.42% (compared to <5% with ZnO nanoparticles) respectively [208,42]. Octahedral (SnO_2) and nanosheet (ZnO) based hierarchical structure performed better than other composites because of their high surface area. For synthesis of such hetero structures, sonochemistry has proved to be more facile and consistent as other methods such as precipitation, hydrothermal, chemical/electrical deposition etc. require long processing time and their inability to produce uniform hetero structures leads to low efficiency. Also, utilizing the physical effect of ultrasound, metal nanoparticles can be simply integrated into such hetero structures to improve their conductivity. Inclusion of noble metals helps prevent photoexcited electrons/holes from recombining and increase the lifetime of electron–hole pair, ultimately increasing efficiency of such hetero structure based solar cells. Kim et al. report on mixing ZnO with Au nanoparticles, while Liu *el al.* report on coating ZnO onto the surface of Ag nanowires [209,210]. In case of Au–ZnO hetero mixture, uniform distribution of Au on ZnO was pivotal in determining their solar cell performance. Therefore, clustering and non-uniform dispersion suffered with sputtering, solvothermal, hydrothermal method etc., had to be rectified, which called for the need of sonochemistry [209].

ZnO and TiO_2 are two widely used materials in making DSSC, because of their proven photocatalytic property, chemical stability, biodegradability and essentially – inexpensive and innocuous nature [42,93,162,167]. However, poor electron mobility in TiO_2 and degrading photocatalytic activity of ZnO often compromises the efficiency of their individual systems. Using a benign solution-based method, a combination of sonochemistry and precipitation, ZnO and TiO_2 based hetero structure has shown to work in synergy to overcome their individual limitations [166]. Such synergistic effect helped stabilize the cell, which is a concerning factor as dye based system deteriorates rapidly with time and use. However, the major problem with DSSC still lies in its electrode configuration, as the requirement to have a transparent electrode hampers the flow of electron, as transparent materials are poor conductors. Therefore, commonly used transparent oxides such as: indium tin oxide (ITO)/glass and fluorine tin oxide (FTO)/glass inevitably hinders electron transport and DSSC efficiency [211]. However, with the emerging of materials such as graphene, nanotubes etc., which are good transparent conductors, efficiency of DSSCs can be further improved. In addition to DSSC and use of Zn and Ti, Cu based hetero structures have also been used in making solar cell – thin film solar cell (TFSC) that offer higher stability than DSSC but with a slight compromise in efficiency, lowering as much as 2.62% [212]. Use of ultrasound for the synthesis of Cu(In or Ga)(S or $Se)_2$ hetero structure, expedites the process and also obviates the common need of stabilizers. Thin film solar cells offer consistent efficiency and stability, but their throughput is too low for practical consideration. On the other hand, silicon based solar cells boast higher efficiency but require direct sunlight to work effectively and impose high fabrication cost, while quantum-dot solar cells are yet to fulfill their potential and high theoretical efficiency (~44%). Hence, DSSCs for their easy and inexpensive manufacturing, standard efficiency, and ability to work at low light condition or indirect sunlight are useful for practical applications and have been synthesized extensively using sonochemistry [211].

5. Conclusion

Region with temperature as high as the surface of our sun and pressure as much as 100 MPa develops at the core of a millimeter sized acoustic bubble to facilitate chemical reactions. Utilizing such extraordinary conditions presented naturally by the acoustic bubbles, extensive range of nanomaterials have been synthesized sonochemically without the aid of any elaborate and expensive equipment or facility. Sonochemistry strives to alleviate exactions and simplify material processing. Metal, polymer, protein, graphene, liquid-filled spheres and many such new and uncommon materials continue to unleash to offer new applications or improve existing ones. Use of sonochemistry is, however, not merely limited to processing of such nanomaterials, but also, in rendering them useful for improved applications. From catalysis, cleaning, sensing, solar energy harvesting to targeted drug delivery, disease treatment, body imaging etc., scope of sonochemistry expands over various fields of science and technology, and continues to be consistent with the current trend. Sonochemistry shows to not only avail contemporary research and processes, but in some instances, has proved to be a better technique than the conventional and matured ones. This survey incorporates the significant contributions and advancements, in addition to the obvious discussion on nanomaterial synthesis.

The opportunities sonochemistry sets up are as exciting as the process, and are imminently realizable. Understanding the mutual effect of input parameters can not only assure control over nanomaterial growth, but also help grow specific materials and unlock new applications. Sonochemically synthesized catalytic metal nanoparticles used in purification, can be furthered to autonomously rectify waste and pollution. Precise drug delivery with the help of sonochemically synthesized protein microcapsules has shown encouraging result in case of tumor treatment, and with the active ongoing research can soon be applicable for other medical conditions. Similarly, the facile sonochemical processing of graphene, carbon nanotubes etc. can help achieve the immense potential these materials promise if performed in large scale. Sonochemistry reaches out even farther for its ability to use different substrates to grow such expedient materials. ZnO nanoparticles synthesized sonochemically on paper and fabrics such as cotton and nylon forecast the advancing smart textile industry. The effective antimicrobial property of ZnO and its UV screening, given its biocompatibility, will not only help improve our health standard but also the textiles we use in daily basis. Given the opportunity, our group is working dedicatedly towards making wearable, portable and real-time biosensor that enables constant monitoring of a person's health. With sonochemistry, possibilities lay endlessly for aspiring researchers.

References

[1] T. Tsakalakos, I.A. Ovid'ko, A.K. Vasudevan, Nanostructures: Synthesis, Functional Properties and Applications, Springer Science & Business Media, 2003.
[2] Y. Xia, P. Yang, Y. Sun, Y. Wu, B. Mayers, B. Gates, Y. Yin, F. Kim, H. Yan, One-dimensional nanostructures: synthesis, characterization, and applications, Adv. Mater. 15 (5) (2003) 353–389.
[3] W.T. Richards, A.L. Loomis, The chemical effects of high frequency sound waves I. A preliminary survey, J. Am. Chem. Soc. 49 (12) (1927) 3086–3100.
[4] M.S. Plesset, A. Prosperetti, Bubble dynamics and cavitation, Annu. Rev. Fluid Mech. 9 (1) (1977) 145–185.
[5] T.G. Leighton, The acoustic bubble, J. Acoust. Soc. Am. 96 (4) (1994) 2616.
[6] K.S. Suslick, Sonochemistry, Science 247 (4949) (1990) 1439–1445 (80-.).
[7] K.S. Suslick, D.J. Flannigan, Inside a collapsing bubble: sonoluminescence and the conditions during cavitation, Annu. Rev. Phys. Chem. 59 (2008) 659–683.
[8] K.S. Suslick, N.C. Eddingsaas, D.J. Flannigan, S.D. Hopkins, H. Xu, Extreme conditions during multibubble cavitation: sonoluminescence as a spectroscopic probe, Ultrason. Sonochem. 18 (4) (2011) 842–846.
[9] J.H. Bang, K.S. Suslick, Applications of ultrasound to the synthesis of nanostructured materials, Adv. Mater. 22 (10) (2010) 1039–1059.
[10] H. Xu, B.W. Zeiger, K.S. Suslick, Sonochemical synthesis of nanomaterials, Chem. Soc. Rev. 42 (7) (2013) 2555–2567.
[11] D.J. Flannigan, K.S. Suslick, Plasma formation and temperature measurement during single-bubble cavitation, Nature 434 (7029) (2005) 52–55.
[12] Y.T. Didenko, W.B. McNamara, K.S. Suslick, Molecular emission from single-bubble sonoluminescence, Nature 407 (6806) (2000) 877–879.
[13] D.J. Flannigan, K.S. Suslick, Plasma line emission during single-bubble cavitation, Phys. Rev. Lett. 95 (4) (2005).
[14] N.C. Eddingsaas, K.S. Suslick, Evidence for a plasma core during multibubble sonoluminescence in sulfuric acid, J. Am. Chem. Soc. 129 (13) (2007) 3838–3839.
[15] R.P. Taleyarkhan, C.D. West, J.S. Cho, R.T. Lahey, R.I. Nigmatulin, R.C. Block, Evidence for nuclear emissions during acoustic cavitation, Science 295 (5561) (2002) 1868–1873.

[16] K.S. Suslick, S.-B. Choe, A.A. Cichowlas, M.W. Grinstaff, Sonochemical synthesis of amorphous iron, Nature 353 (6343) (1991) 414–416.
[17] Y. Koltypin, G. Katabi, X. Cao, R. Prozorov, A. Gedanken, Sonochemical preparation of amorphous nickel, J. Non Cryst. Solids 201 (1–2) (1996) 159–162.
[18] T. Hyeon, M. Fang, K.S. Suslick, Nanostructured molybdenum carbide: sonochemical synthesis and catalytic properties, J. Am. Chem. Soc. 118 (23) (1996) 5492–5493.
[19] K.S. Suslick, T. Hyeon, M. Fang, Nanostructured materials generated by high-intensity ultrasound: sonochemical synthesis and catalytic studies, Chem. Mater. 8 (8) (1996) 2172–2179.
[20] M.M. Mdleleni, T. Hyeon, K.S. Suslick, Sonochemical synthesis of nanostructured molybdenum sulfide, J. Am. Chem. Soc. 120 (24) (1998) 6189–6190.
[21] P.K. Vabbina, M. Karabiyik, C. Al-Amin, N. Pala, S. Das, W. Choi, T. Saxena, M. Shur, Controlled synthesis of single-crystalline ZnO nanoflakes on arbitrary substrates at ambient conditions, Part. Part. Syst. Charact. 31 (2) (2014) 190–194.
[22] J.H. Bang, K.S. Suslick, Applications of ultrasound to the synthesis of nanostructured materials, Adv. Mater. 22 (10) (2010) 1039–1059.
[23] S. Doktycz, K. Suslick, Interparticle collisions driven by ultrasound, Science 247 (4946) (1990) 1067–1069 (80-.).
[24] B.W. Zeiger, K.S. Suslick, Sonofragmentation of molecular crystals, J. Am. Chem. Soc. 133 (37) (2011) 14530–14533.
[25] L.M. Viculis, J.J. Mack, R.B. Kaner, A chemical route to carbon nanoscrolls, Science 299 (5611) (2003) 1361.
[26] H. Xu, K.S. Suslick, Sonochemical preparation of functionalized graphenes, J. Am. Chem. Soc. 133 (24) (2011) 9148–9151.
[27] Y. Wang, C. Zhou, W. Wang, Y. Zhao, Preparation of two dimensional atomic crystals BN, WS_2, and MoS_2 by supercritical CO_2 assisted with ultrasound, Ind. Eng. Chem. Res. 52 (11) (2013) 4379–4382.
[28] N.A. Dhas, K.S. Suslick, Sonochemical preparation of hollow nanospheres and hollow nanocrystals, J. Am. Chem. Soc. 127 (8) (2005) 2368–2369.
[29] M. Lotya, Y. Hernandez, P.J. King, R.J. Smith, V. Nicolosi, L.S. Karlsson, F.M. Blighe, S. De, Z. Wang, I.T. McGovern, G.S. Duesberg, J.N. Coleman, Liquid phase production of graphene by exfoliation of graphite in surfactant/water solutions, J. Am. Chem. Soc. 131 (10) (2009) 3611–3620.
[30] W. Zhang, W. He, X. Jing, Preparation of a stable graphene dispersion with high concentration by ultrasound, J. Phys. Chem. B 114 (32) (2010) 10368–10373.
[31] K.S. Suslick, M.W. Grinstaff, Protein microencapsulation of nonaqueous liquids, J. Am. Chem. Soc. 112 (21) (1990) 7807–7809.
[32] I. Perelshtein, G. Applerot, N. Perkas, G. Guibert, S. Mikhailov, A. Gedanken, Sonochemical coating of silver nanoparticles on textile fabrics (nylon, polyester and cotton) and their antibacterial activity, Nanotechnology 19 (24) (2008) 245705.
[33] I. Perelshtein, G. Applerot, N. Perkas, E. Wehrschetz-Sigl, A. Hasmann, G.M. Guebitz, A. Gedanken, Antibacterial properties of an in situ generated and simultaneously deposited nanocrystalline ZnO on fabrics, ACS Appl. Mater. Interfaces 1 (2) (2009) 361–366.
[34] R. Gottesman, S. Shukla, N. Perkas, L.A. Solovyov, Y. Nitzan, A. Gedanken, Sonochemical coating of paper by microbiocidal silver nanoparticles, Langmuir 27 (2) (2011) 720–726.
[35] K.S. Suslick, P.F. Schubert, J.W. Goodale, Sonochemistry and sonocatalysis of iron carbonyls, J. Am. Chem. Soc. 103 (24) (1981) 7342–7344.
[36] K.S. Suslick, J.J. Gawienowski, P.F. Schubert, H.H. Wang, Alkane sonochemistry, J. Phys. Chem. 87 (13) (1983) 2299–2301.
[37] K.S. Suslick, J.W. Goodale, P.F. Schubert, H.H. Wang, Sonochemistry and sonocatalysis of metal carbonyls, J. Am. Chem. Soc. 105 (18) (1983) 5781–5785.
[38] K.S. Suslick, The chemical effects of ultrasound, Sci. Am. 260 (2) (1989) 80–86.
[39] F.J.J. Toublan, S. Boppart, K.S. Suslick, Tumor targeting by surface-modified protein microspheres, J. Am. Chem. Soc. 128 (11) (2006) 3472–3473.
[40] A.G. Webb, M. Wong, K.J. Kolbeck, R. Magin, K.S. Suslick, Sonochemically produced fluorocarbon microspheres: a new class of magnetic resonance imaging agent, J. Magn. Reson. Imaging 6 (4) (1996) 675–683.
[41] R.V. Kumar, Y. Diamant, A. Gedanken, Sonochemical synthesis and characterization of nanometer-size transition metal oxides from metal acetates, Chem. Mater. 12 (8) (2000) 2301–2305.
[42] Y. Shi, C. Zhu, L. Wang, C. Zhao, W. Li, K.K. Fung, T. Ma, A. Hagfeldt, N. Wang, Ultrarapid sonochemical synthesis of ZnO hierarchical structures: From fundamental research to high efficiencies up to 6.42% for quasi-solid dye-sensitized solar cells, Chem. Mater. 25 (6) (2013) 1000–1012.
[43] Y. Xu, P.E. Pehrsson, L. Chen, R. Zhang, W. Zhao, Double-stranded DNA single-walled carbon nanotube hybrids for optical hydrogen peroxide and glucose sensing, J. Phys. Chem. C 111 (24) (2007) 8638–8643.
[44] Y. Mizukoshi, T. Fujimoto, Y. Nagata, R. Oshima, Y. Maeda, Characterization and catalytic activity of core–shell structured gold/palladium bimetallic nanoparticles synthesized by the sonochemical method, J. Phys. Chem. B 104 (25) (2000) 6028–6032.
[45] H.-C. Pan, F.-P. Liang, C.-J. Mao, J.-J. Zhu, H.-Y. Chen, Highly luminescent zinc(II)-bis(8-hydroxyquinoline) complex nanorods: sonochemical synthesis, characterizations, and protein sensing, J. Phys. Chem. B 111 (20) (2007) 5767–5772.
[46] N.A. Tsochatzidis, P. Guiraud, A.M. Wilhelm, H. Delmas, Determination of velocity, size and concentration of ultrasonic cavitation bubbles by the phase-Doppler technique, Chem. Eng. Sci. 56 (5) (2001) 1831–1840.
[47] W. Lauterborn, C.-D. Ohl, Cavitation bubble dynamics, Ultrason. Sonochem. 4 (2) (1997) 65–75.
[48] L. Zhang, V. Belova, H. Wang, W. Dong, H. Möhwald, Controlled cavitation at nano/microparticle surfaces, Chem. Mater. 26 (7) (2014) 2244–2248.
[49] S. Merouani, O. Hamdaoui, Y. Rezgui, M. Guemini, Effects of ultrasound frequency and acoustic amplitude on the size of sonochemically active bubbles-theoretical study, Ultrason. Sonochem. 20 (3) (2013) 815–819.
[50] A.E. Kandjani, M.F. Tabriz, B. Pourabbas, Sonochemical synthesis of ZnO nanoparticles: the effect of temperature and sonication power, Mater. Res. Bull. 43 (3) (2008) 645–654.
[51] K. Okitsu, M. Ashokkumar, F. Grieser, Sonochemical synthesis of gold nanoparticles: effects of ultrasound frequency, J. Phys. Chem. B 109 (44) (2005) 20673–20675.
[52] S.-H. Jung, E. Oh, K.-H. Lee, Y. Yang, C.G. Park, W. Park, S.-H. Jeong, Sonochemical preparation of shape-selective ZnO nanostructures, Cryst. Growth Des. 8 (1) (2008) 265–269.
[53] T. Tuziuti, K. Yasui, K. Kato, Influence of degree of gas saturation on multibubble sonoluminescence intensity, J. Phys. Chem. A 115 (20) (2011) 5089–5093.
[54] W. Cui, S. Qi, W. Chen, C. Zhou, J. Tu, Effect of alcohol on single-bubble sonoluminescence, Phys. Rev. E 85 (2) (2012) 026304.
[55] J. Lee, M. Ashokkumar, S. Kentish, F. Grieser, Effect of alcohols on the initial growth of multibubble sonoluminescence, J. Phys. Chem. B 110 (34) (2006) 17282–17285.
[56] T. Leong, S. Wu, S. Kentish, M. Ashokkumar, Growth of bubbles by rectified diffusion in aqueous surfactant solutions, J. Phys. Chem. C 114 (47) (2010) 20141–20145.
[57] A. Henglein, D. Herburger, M. Gutierrez, Sonochemistry: some factors that determine the ability of a liquid to cavitate in an ultrasonic field, J. Phys. Chem. 96 (3) (1992) 1126–1130.
[58] J.P. Lorimer, T.J. Mason, Sonochemistry. Part 1 – the physical aspects, Chem. Soc. Rev. 16 (1987) 239.
[59] T. Leong, K. Yasui, K. Kato, D. Harvie, M. Ashokkumar, S. Kentish, Effect of surfactants on single bubble sonoluminescence behavior and bubble surface stability, Phys. Rev. E 89 (4) (2014) 043007.
[60] M. Ashokkumar, R. Hall, P. Mulvaney, F. Grieser, Sonoluminescence from aqueous alcohol and surfactant solutions, J. Phys. Chem. B 101 (50) (1997) 10845–10850.
[61] A. Brotchie, T. Statham, M. Zhou, L. Dharmarathne, F. Grieser, M. Ashokkumar, Acoustic bubble sizes, coalescence, and sonochemical activity in aqueous electrolyte solutions saturated with different gases, Langmuir 26 (15) (2010) 12690–12695.
[62] Y. Mizukoshi, K. Okitsu, Y. Maeda, T.A. Yamamoto, R. Oshima, Y. Nagata, Sonochemical preparation of bimetallic nanoparticles of gold/palladium in aqueous solution, J. Phys. Chem. B 101 (36) (1997) 7033–7037.
[63] J. Lee, S. Kentish, T.J. Matula, M. Ashokkumar, Effect of surfactants on inertial cavitation activity in a pulsed acoustic field, J. Phys. Chem. B 109 (35) (2005) 16860–16865.
[64] J. Lee, S. Kentish, M. Ashokkumar, Effect of surfactants on the rate of growth of an air bubble by rectified diffusion, J. Phys. Chem. B 109 (30) (2005) 14595–14598.
[65] R. Tronson, M. Ashokkumar, F. Grieser, Comparison of the effects of water-soluble solutes on multibubble sonoluminescence generated in aqueous solutions by 20- and 515-kHz pulsed ultrasound, J. Phys. Chem. B 106 (42) (2002) 11064–11068.
[66] J. Lee, M. Ashokkumar, S. Kentish, F. Grieser, Determination of the size distribution of sonoluminescence bubbles in a pulsed acoustic field, J. Am. Chem. Soc. 127 (48) (2005) 16810–16811.
[67] F. Mohandes, M. Salavati-Niasari, Sonochemical synthesis of silver vanadium oxide micro/nanorods: solvent and surfactant effects, Ultrason. Sonochem. 20 (1) (2013) 354–365.
[68] R. Vijaya Kumar, R. Elgamiel, Y. Diamant, A. Gedanken, J. Norwig, Sonochemical preparation and characterization of nanocrystalline copper oxide embedded in poly(vinyl alcohol) and its effect on crystal growth of copper oxide, Langmuir 17 (5) (2001) 1406–1410.
[69] K.V.P.M. Shafi, A. Ulman, X. Yan, N.-L. Yang, C. Estournès, H. White, M. Rafailovich, Sonochemical synthesis of functionalized amorphous iron oxide nanoparticles, Langmuir 17 (16) (2001) 5093–5097.
[70] A. Nemamcha, J.-L. Rehspringer, D. Khatmi, Synthesis of palladium nanoparticles by sonochemical reduction of palladium(II) nitrate in aqueous solution, J. Phys. Chem. B 110 (1) (2006) 383–387.
[71] G.J. Price, M. Ashokkumar, F. Grieser, Sonoluminescence quenching of organic compounds in aqueous solution: frequency effects and implications for sonochemistry, J. Am. Chem. Soc. 126 (9) (2004) 2755–2762.
[72] S. Merouani, O. Hamdaoui, Y. Rezgui, M. Guemini, Effects of ultrasound frequency and acoustic amplitude on the size of sonochemically active bubbles – theoretical study, Ultrason. Sonochem. 20 (3) (2013) 815–819.
[73] A. Brotchie, F. Grieser, M. Ashokkumar, Effect of power and frequency on bubble-size distributions in acoustic cavitation, Phys. Rev. Lett. 102 (8) (2009) 084302.
[74] E. Ciawi, J. Rae, M. Ashokkumar, F. Grieser, Determination of temperatures within acoustically generated bubbles in aqueous solutions at different ultrasound frequencies, J. Phys. Chem. B 110 (27) (2006) 13656–13660.
[75] S. Koda, T. Kimura, T. Kondo, H. Mitome, A standard method to calibrate sonochemical efficiency of an individual reaction system, Ultrason. Sonochem. 10 (3) (2003) 149–156.

[76] A. Hassanjani-Roshan, S.M. Kazemzadeh, M.R. Vaezi, A. Shokuhfar, The effect of sonication power on the sonochemical synthesis of titania nanoparticles, J. Ceram. Process. Res. 12 (3) (2011) 299–303.
[77] R. Wahab, S.G. Ansari, Y.-S. Kim, H.-K. Seo, H.-S. Shin, Room temperature synthesis of needle-shaped ZnO nanorods via sonochemical method, Appl. Surf. Sci. 253 (18) (2007) 7622–7626.
[78] D.M.D.J. Singh, T. Pradeep, J. Bhattacharjee, U.V. Waghmare, Closed-cage clusters in the gaseous and condensed phases derived from sonochemically synthesized MoS_2 nanoflakes, J. Am. Soc. Mass Spectrom. 18 (12) (2007) 2191–2197.
[79] H. Wang, Y.-N. Lu, J.-J. Zhu, H.-Y. Chen, Sonochemical fabrication and characterization of stibnite nanorods, Inorg. Chem. 42 (20) (2003) 6404–6411.
[80] F. Xiao, F. Zhao, Y. Zhang, G. Guo, B. Zeng, Ultrasonic electrodeposition of gold–platinum alloy nanoparticles on ionic liquid-chitosan composite film and their application in fabricating nonenzyme hydrogen peroxide sensors, J. Phys. Chem. C 113 (3) (2009) 849–855.
[81] F. Xiao, F. Zhao, D. Mei, Z. Mo, B. Zeng, Nonenzymatic glucose sensor based on ultrasonic-electrodeposition of bimetallic PtM (M = Ru, Pd and Au) nanoparticles on carbon nanotubes-ionic liquid composite film, Biosens. Bioelectron. 24 (12) (2009) 3481–3486.
[82] T. Prozorov, R. Prozorov, K.S. Suslick, High velocity interparticle collisions driven by ultrasound, J. Am. Chem. Soc. 126 (43) (2004) 13890–13891.
[83] M.D. Kass, Ultrasonically induced fragmentation and strain in alumina particles, Mater. Lett. 42 (4) (2000) 246–250.
[84] Y. Wang, C. Zhou, W. Wang, Y. Zhao, Preparation of two dimensional atomic crystals BN, WS_2, and MoS_2 by supercritical CO_2 assisted with ultrasound, Ind. Eng. Chem. Res. 52 (11) (2013) 4379–4382.
[85] K.S. Suslick, The chemical effects of ultrasound, Sci. Am. 260 (2) (1989) 80–86.
[86] A.C. Barton, S.D. Collyer, F. Davis, D.D. Gornall, K.A. Law, E.C.D. Lawrence, D.W. Mills, S. Myler, J.A. Pritchard, M. Thompson, S.P.J. Higson, Sonochemically fabricated microelectrode arrays for biosensors offering widespread applicability: part I, Biosens. Bioelectron. 20 (2) (2004) 328–337.
[87] C. Cau, S.I. Nikitenko, Mechanism of W(CO)6 sonolysis in diphenylmethane, Ultrason. Sonochem. 19 (3) (2012) 498–502.
[88] S. Anandan, G.-J. Lee, J.J. Wu, Sonochemical synthesis of CuO nanostructures with different morphology, Ultrason. Sonochem. 19 (3) (2012) 682–686.
[89] D.N. Srivastava, N. Perkas, A. Gedanken, I. Felner, Sonochemical synthesis of mesoporous iron oxide and accounts of its magnetic and catalytic properties, J. Phys. Chem. B 106 (8) (2002) 1878–1883.
[90] I.B. Johns, E.A. McElhill, J.O. Smith, Thermal stability of some organic compounds, J. Chem. Eng. Data 7 (2) (1962) 277–281.
[91] S.A. Wieczorek, R. Kobayashi, Vapor pressure measurements of diphenylmethane, thianaphthene, and bicyclohexyl at elevated temperatures, J. Chem. Eng. Data 25 (4) (1980) 302–305.
[92] R. Chellappa, D. Chandra, Assessment of vapor pressure data of solid metal carbonyls, J. Chem. Thermodyn. 37 (4) (2005) 377–387.
[93] Z.L. Wang, Zinc oxide nanostructures: growth, properties and applications, J. Phys.: Condens. Matter 16 (25) (2004) R829–R858.
[94] D. Aurbach, A. Nimberger, B. Markovsky, E. Levi, E. Sominski, A. Gedanken, Nanoparticles of SnO produced by sonochemistry as anode materials for rechargeable lithium batteries, Chem. Mater. 14 (10) (2002) 4155–4163.
[95] S. Zhu, J. Guo, J. Dong, Z. Cui, T. Lu, C. Zhu, D. Zhang, J. Ma, Sonochemical fabrication of Fe_3O_4 nanoparticles on reduced graphene oxide for biosensors, Ultrason. Sonochem. 20 (3) (2013) 872–880.
[96] M.R. DuBois, Catalytic applications of transition-metal complexes with sulfide ligands, Chem. Rev. (Washington, DC, United States) 89 (1) (1989) 1–9.
[97] R.B. Levy, M. Boudart, Platinum-like behavior of tungsten carbide in surface catalysis, Science 181 (4099) (1973) 547–549.
[98] S.I. Nikitenko, Y. Koltypin, I. Felner, I. Yeshurun, A.I. Shames, J.Z. Jiang, V. Markovich, G. Gorodetsky, A. Gedanken, Tailoring the properties of Fe–Fe_3C nanocrystalline particles prepared by sonochemistry, J. Phys. Chem. B 108 (23) (2004) 7620–7626.
[99] L. Machala, R. Zboril, A. Gedanken, Amorphous iron(III) oxide – a review, J. Phys. Chem. B 111 (16) (2007) 4003–4018.
[100] J.D. Oxley, M.M. Mdleleni, K.S. Suslick, Hydrodehalogenation with sonochemically prepared Mo_2C and W_2C, Catal. Today 88 (3–4) (2004) 139–151.
[101] J.J.H.B. Sattler, J. Ruiz-Martinez, E. Santillan-Jimenez, B.M. Weckhuysen, Catalytic dehydrogenation of light alkanes on metals and metal oxides, Chem. Rev. 114 (20) (2014) 10613–10653.
[102] M.J. Hudson, J.W. Peckett, P.J.F. Harris, Low-temperature sol–gel preparation of ordered nanoparticles of tungsten carbide/oxide, Ind. Eng. Chem. Res. 44 (15) (2005) 5575–5578.
[103] C. Giordano, C. Erpen, W. Yao, M. Antonietti, Synthesis of Mo and W carbide and nitride nanoparticles via a simple 'urea glass' route, Nano Lett. 8 (12) (2008) 4659–4663.
[104] P.K. Shen, S. Yin, Z. Li, C. Chen, Preparation and performance of nanosized tungsten carbides for electrocatalysis, Electrochim. Acta 55 (27) (2010) 7969–7974.
[105] F. Alonso, I.P. Beletskaya, M. Yus, Metal-mediated reductive hydrodehalogenation of organic halides, Chem. Rev. 102 (11) (2002) 4009–4092.
[106] B. Dhandapani, S.T. Oyama, Novel catalysts for selective dehalogenation of CCl2F2(CFC 12), Catal. Lett. 35 (3–4) (1995) 353–360.
[107] L. Delannoy, J.-M. Giraudon, P. Granger, L. Leclercq, G. Leclercq, Group VI transition metal carbides as alternatives in the hydrodechlorination of chlorofluorocarbons, Catal. Today 59 (3–4) (2000) 231–240.
[108] C.D. Vecitis, Y. Wang, J. Cheng, H. Park, B.T. Mader, M.R. Hoffmann, Sonochemical degradation of perfluorooctanesulfonate in aqueous film-forming foams, Environ. Sci. Technol. 44 (1) (2010) 432–438.
[109] A.K. Shriwas, P.R. Gogate, Intensification of degradation of 2,4,6-trichlorophenol using sonochemical reactors: understanding mechanism and scale-up aspects, Ind. Eng. Chem. Res. 50 (16) (2011) 9601–9608.
[110] Y.G. Adewuyi, Sonochemistry: environmental science and engineering applications, Ind. Eng. Chem. Res. 40 (22) (2001) 4681–4715.
[111] M. Hoffmann, Application of ultrasonic irradiation for the degradation of chemical contaminants in water, Ultrason. Sonochem. 3 (3) (1996) S163–S172.
[112] S. Goskonda, W. James Catallo, T. Junk, Sonochemical degradation of aromatic organic pollutants, Waste Manag. 22 (3) (2002) 351–356.
[113] A. Tiehm, U. Neis, Ultrasonic dehalogenation and toxicity reduction of trichlorophenol, Ultrason. Sonochem. 12 (1–2) (2005) 121–125.
[114] N. Serpone, R. Terzian, H. Hidaka, E. Pelizzetti, Ultrasonic induced dehalogenation and oxidation of 2-, 3-, and 4-chlorophenol in air-equilibrated aqueous media. similarities with irradiated semiconductor particulates, J. Phys. Chem. 98 (10) (1994) 2634–2640.
[115] Y. Koltypin, S.I. Nikitenko, A. Gedanken, The sonochemical preparation of tungsten oxide nanoparticles, J. Mater. Chem. 12 (4) (2002) 1107–1110.
[116] S.I. Nikitenko, Y. Koltypin, Y. Mastai, M. Koltypin, A. Gedanken, Sonochemical synthesis of tungsten sulfide nanorods, J. Mater. Chem. 12 (5) (2002) 1450–1452.
[117] A.-H. Lu, E.L. Salabas, F. Schüth, Magnetic nanoparticles: synthesis, protection, functionalization, and application, Angew. Chem. Int. Ed. Engl. 46 (8) (2007) 1222–1244.
[118] Y. Zhu, L.P. Stubbs, F. Ho, R. Liu, C.P. Ship, J.A. Maguire, N.S. Hosmane, Magnetic nanocomposites: a new perspective in catalysis, ChemCatChem 2 (4) (2010) 365–374.
[119] R. Kaur, A. Hasan, N. Iqbal, S. Alam, M.K. Saini, S.K. Raza, Synthesis and surface engineering of magnetic nanoparticles for environmental cleanup and pesticide residue analysis: a review, J. Sep. Sci. 37 (14) (2014) 1805–1825.
[120] S.Y. Chou, M.S. Wei, P.R. Krauss, P.B. Fischer, Single-domain magnetic pillar array of 35 nm diameter and 65 Gbits/in.2 density for ultrahigh density quantum magnetic storage, J. Appl. Phys. 76 (10) (1994) 6673.
[121] S.I. Nikitenko, Y. Koltypin, V. Markovich, E. Rozenberg, G. Gorodetsky, A. Gedanken, Synthesis of air-stable iron–iron carbide nanocrystalline particles showing very high saturation magnetization, IEEE Trans. Magn. 38 (5) (2002) 2592–2594.
[122] S.I. Nikitenko, Y. Koltypin, O. Palchik, I. Felner, X.N. Xu, A. Gedanken, Synthesis of highly magnetic, air-stable iron–iron carbide nanocrystalline particles by using power ultrasound, Angew. Chem. Int. Ed. Engl. 40 (23) (2001) 4447–4449.
[123] Y. Koltypin, N. Perkas, A. Gedanken, Commercial edible oils as new solvents for ultrasonic synthesis of nanoparticles: the preparation of air stable nanocrystalline iron particles, J. Mater. Chem. 14 (20) (2004) 2975.
[124] M. Sivakumar, T. Takami, H. Ikuta, A. Towata, K. Yasui, T. Tuziuti, T. Kozuka, D. Bhattacharya, Y. Iida, Fabrication of zinc ferrite nanocrystals by sonochemical emulsification and evaporation: observation of magnetization and its relaxation at low temperature, J. Phys. Chem. B 110 (31) (2006) 15234–15243.
[125] R. Miyatani, Y. Yamada, Y. Kobayashi, Mössbauer study of iron carbide nanoparticles produced by sonochemical synthesis, J. Radioanal. Nucl. Chem. 303 (2) (2014) 1503–1506.
[126] Y. Koltypin, A. Fernandez, T.C. Rojas, J. Campora, P. Palma, R. Prozorov, A. Gedanken, Encapsulation of nickel nanoparticles in carbon obtained by the sonochemical decomposition of $Ni(C_8H_{12})_2$, Chem. Mater. 11 (5) (1999) 1331–1335.
[127] G. Meyer, F.E.C. Scheffer, The properties of nickel carbide, J. Am. Chem. Soc. 75 (2) (1953) (486–486).
[128] P. Jeevanandam, Y. Koltypin, A. Gedanken, Synthesis of nanosized α-nickel hydroxide by a sonochemical method, Nano Lett. 1 (5) (2001) 263–266.
[129] N.A. Dhas, A. Ekhtiarzadeh, K.S. Suslick, Sonochemical preparation of supported hydrodesulfurization catalysts, J. Am. Chem. Soc. 123 (34) (2001) 8310–8316.
[130] Z. Zhong, Y. Mastai, Y. Koltypin, Y. Zhao, A. Gedanken, Sonochemical coating of nanosized nickel on alumina submicrospheres and the interaction between the nickel and nickel oxide with the substrate, Chem. Mater. 11 (9) (1999) 2350–2359.
[131] V.G. Pol, O. Palchik, A. Gedanken, I. Felner, Synthesis of europium oxide nanorods by ultrasound irradiation, J. Phys. Chem. B 106 (38) (2002) 9737–9743.
[132] L. Yin, Y. Wang, G. Pang, Y. Koltypin, A. Gedanken, Sonochemical synthesis of cerium oxide nanoparticles-effect of additives and quantum size effect, J. Colloid Interface Sci. 246 (1) (2002) 78–84.
[133] R. Abu Mukh-Qasem, A. Gedanken, Sonochemical synthesis of stable hydrosol of Fe_3O_4 nanoparticles, J. Colloid Interface Sci. 284 (2) (2005) 489–494.
[134] N.A. Dhas, A. Gedanken, Characterization of sonochemically prepared unsupported and silica-supported nanostructured pentavalent molybdenum oxide, J. Phys. Chem. B 101 (46) (1997) 9495–9503.

[135] S. Laurent, D. Forge, M. Port, A. Roch, C. Robic, L. Vander Elst, R.N. Muller, Magnetic iron oxide nanoparticles: synthesis, stabilization, vectorization, physicochemical characterizations, and biological applications, Chem. Rev. 108 (6) (2008) 2064–2110.

[136] N.A. Dhas, Y. Koltypin, A. Gedanken, Sonochemical preparation and characterization of ultrafine chromium oxide and manganese oxide powders, Chem. Mater. 9 (12) (1997) 3159–3163.

[137] R. Vijayakumar, Y. Koltypin, I. Felner, A. Gedanken, Sonochemical synthesis and characterization of pure nanometer-sized Fe_3O_4 particles, Mater. Sci. Eng. A 286 (1) (2000) 101–105.

[138] Q. Zhang, K. Zhang, D. Xu, G. Yang, H. Huang, F. Nie, C. Liu, S. Yang, CuO nanostructures: synthesis, characterization, growth mechanisms, fundamental properties, and applications, Prog. Mater Sci. 60 (2014) 208–337.

[139] X. Cao, R. Prozorov, Y. Koltypin, G. Kataby, I. Felner, A. Gedanken, Synthesis of pure amorphous Fe_2O_3, J. Mater. Res. 12 (02) (1997) 402–406.

[140] S. Zhang, Y. Zhang, Y. Wang, S. Liu, Y. Deng, Sonochemical formation of iron oxide nanoparticles in ionic liquids for magnetic liquid marble, Phys. Chem. Chem. Phys. 14 (15) (2012) 5132.

[141] T. Gao, Q. Li, T. Wang, Sonochemical synthesis, optical properties, and electrical properties of core/shell-type ZnO nanorod/CdS nanoparticle composites, Chem. Mater. 17 (4) (2005) 887–892.

[142] M. Kristl, M. Drofenik, Sonochemical synthesis of nanocrystalline mercury sulfide, selenide and telluride in aqueous solutions, Ultrason. Sonochem. 15 (5) (2008) 695–699.

[143] M. Jesionek, M. Nowak, P. Szperlich, D. Stró, J. Szala, K. Jesionek, T. Rzychoń, Sonochemical growth of antimony selenoiodide in multiwalled carbon nanotube, Ultrason. Sonochem. 19 (1) (2012) 179–185.

[144] G.S. Wu, X.Y. Yuan, T. Xie, G.C. Xu, L.D. Zhang, Y.L. Zhuang, A simple synthesis route to CdS nanomaterials with different morphologies by sonochemical reduction, Mater. Lett. 58 (5) (2004) 794–797.

[145] K.S. Suslick, M. Fang, T. Hyeon, Sonochemical synthesis of iron colloids, J. Am. Chem. Soc. 118 (47) (1996) 11960–11961.

[146] J. Zhang, J. Du, B. Han, Z. Liu, T. Jiang, Z. Zhang, Sonochemical formation of single-crystalline gold nanobelts, Angew. Chem. 118 (7) (2006) 1134–1137.

[147] A. Sánchez-Iglesias, I. Pastoriza-Santos, J. Pérez-Juste, B. Rodríguez-González, F.J. García de Abajo, L.M. Liz-Marzán, Synthesis and optical properties of gold nanodecahedra with size control, Adv. Mater. 18 (19) (2006) 2529–2534.

[148] H. Liu, X. Zhang, X. Wu, L. Jiang, C. Burda, J.-J. Zhu, Rapid sonochemical synthesis of highly luminescent non-toxic AuNCs and Au@AgNCs and Cu (II) sensing, Chem. Commun. (Camb.) 47 (14) (2011) 4237–4239.

[149] H. Xu, K.S. Suslick, Sonochemical synthesis of highly fluorescent Ag nanoclusters, ACS Nano 4 (6) (2010) 3209–3214.

[150] K. Okitsu, H. Bandow, Sonochemical preparation of ultrafine palladium particles, Chem. Mater. 18 (1996) 315–317.

[151] Y. Mizukoshi, R. Oshima, Y. Maeda, Y. Nagata, Preparation of platinum nanoparticles by sonochemical reduction of the Pt(II) ion, Langmuir 15 (8) (1999) 2733–2737.

[152] Y. Mizukoshi, E. Takagi, H. Okuno, R. Oshima, Y. Maeda, Y. Nagata, Preparation of platinum nanoparticles by sonochemical reduction of the Pt(IV) ions: role of surfactants, Ultrason. Sonochem. 8 (1) (2001) 1–6.

[153] K. Vinodgopal, Y. He, M. Ashokkumar, F. Grieser, Sonochemically prepared platinum–ruthenium bimetallic nanoparticles, J. Phys. Chem. B 110 (9) (2006) 3849–3852.

[154] V.G. Pol, A. Gedanken, J. Calderon-Moreno, Deposition of gold nanoparticles on silica spheres: a sonochemical approach, Chem. Mater. 15 (5) (2003) 1111–1118.

[155] N.A. Dhas, A. Gedanken, Sonochemical synthesis of molybdenum oxide- and molybdenum carbide-silica nanocomposites, Chem. Mater. 9 (12) (1997) 3144–3154.

[156] S. Ramesh, Y. Koltypin, R. Prozorov, A. Gedanken, Sonochemical deposition and characterization of nanophasic amorphous nickel on silica microspheres, Chem. Mater. 9 (2) (1997) 546–551.

[157] K.V.P.M. Shafi, Y. Koltypin, A. Gedanken, R. Prozorov, J. Balogh, J. Lendvai, I. Felner, Sonochemical preparation of nanosized amorphous $NiFe_2O_4$ particles, J. Phys. Chem. B 101 (33) (1997) 6409–6414.

[158] K.V.P.M. Shafi, A. Ulman, X. Yan, N.-L. Yang, C. Estournès, H. White, M. Rafailovich, A. Gedanken, R. Prozorov, J. Balogh, R.B. Goldfarb, I. Felner, Y. Koltypin, X. Cao, D. Kaptas, Sonochemical preparation and size-dependent properties of nanostructured $CoFe_2O_4$ particles, J. Mater. Chem. 7 (11) (1997) 3445–3450.

[159] S.W. Lee, S. Bae, Y. Takemura, I.B. Shim, T.M. Kim, J. Kim, H.J. Lee, S. Zurn, C.S. Kim, Self-heating characteristics of cobalt ferrite nanoparticles for hyperthermia application, J. Magn. Magn. Mater. 310 (2 Suppl, Part 3) (2007) 2868–2870.

[160] M.H. Sousa, F.A. Tourinho, J. Depeyrot, G.J. da Silva, M.C.F.L. Lara, New electric double-layered magnetic fluids based on copper, nickel, and zinc ferrite nanostructures, J. Phys. Chem. B 105 (2001) 1168–1175.

[161] V. Šepelák, I. Bergmann, A. Feldhoff, P. Heitjans, F. Krumeich, D. Menzel, F.J. Litterst, S.J. Campbell, K.D. Becker, Nanocrystalline nickel ferrite, $NiFe_2O_4$: mechanosynthesis, nonequilibrium cation distribution, canted spin arrangement, and magnetic behavior, J. Phys. Chem. C 111 (13) (2007) 5026–5033.

[162] A. Mclaren, T. Valdes-Solis, G. Li, S.C. Tsang, Shape and size effects of ZnO nanocrystals on photocatalytic activity, J. Am. Chem. Soc. 131 (35) (2009) 12540–12541.

[163] P. Banerjee, S. Chakrabarti, S. Maitra, B.K. Dutta, Zinc oxide nano-particles – sonochemical synthesis, characterization and application for photo-remediation of heavy metal, Ultrason. Sonochem. 19 (1) (2012) 85–93.

[164] A.P. Nayak, A.M. Katzenmeyer, J.-Y. Kim, M.K. Kwon, Y. Gosho, M.S. Islam, Purely sonochemical route for oriented zinc oxide nanowire growth on arbitrary substrate, Proc. SPIE 7683 (2010) (768312–768312–8).

[165] W. Li, Z. Wu, J. Wang, A.A. Elzatahry, D. Zhao, A perspective on mesoporous TiO_2 materials, Chem. Mater. 26 (1) (2014) 287–298.

[166] C. Cheng, A. Amini, C. Zhu, Z. Xu, H. Song, N. Wang, Enhanced photocatalytic performance of TiO_2–ZnO hybrid nanostructures, Sci. Rep. 4 (2014) 4181.

[167] Y. Wang, X. Tang, L. Yin, W. Huang, Y. Rosenfeld Hacohen, A. Gedanken, Sonochemical synthesis of mesoporous titanium oxide with wormhole-like framework structures, Adv. Mater. 12 (16) (2000) 1183–1186.

[168] J.C. Yu, L. Zhang, J. Yu, Direct sonochemical preparation and characterization of highly active mesoporous TiO_2 with a bicrystalline framework, Chem. Mater. 14 (11) (2002) 4647–4653.

[169] D.M. Antonelli, Synthesis of phosphorus-free mesoporous titania via templating with amine surfactants, Microporous Mesoporous Mater. 30 (2–3) (1999) 315–319.

[170] N.M. Pugno, On the strength of the carbon nanotube-based space elevator cable: from nanomechanics to megamechanics, J. Phys.: Condens. Matter 18 (33) (2006) S1971–S1990.

[171] S.H. Jeong, J.H. Ko, J.B. Park, W. Park, A sonochemical route to single-walled carbon nanotubes under ambient conditions, J. Am. Chem. Soc. 126 (49) (2004) 15982–15983.

[172] I.W. Chiang, B.E. Brinson, A.Y. Huang, P.A. Willis, M.J. Bronikowski, J.L. Margrave, R.E. Smalley, R.H. Hauge, Purification and characterization of single-wall carbon nanotubes (SWNTs) obtained from the gas-phase decomposition of CO (HiPco process), J. Phys. Chem. B 105 (35) (2001) 8297–8301.

[173] H. Hu, B. Zhao, M.E. Itkis, R.C. Haddon, Nitric acid purification of single-walled carbon nanotubes, J. Phys. Chem. B 107 (50) (2003) 13838–13842.

[174] X.-H. Sun, C.-P. Li, N.-B. Wong, C.-S. Lee, S.-T. Lee, B.-K. Teo, Templating effect of hydrogen-passivated silicon nanowires in the production of hydrocarbon nanotubes and nanoonions via sonochemical reactions with common organic solvents under ambient conditions, J. Am. Chem. Soc. 124 (50) (2002) 14856–14857.

[175] C.P. Li, B.K. Teo, X.H. Sun, N.B. Wong, S.T. Lee, Hydrocarbon and carbon nanostructures produced by sonochemical reactions of organic solvents on hydrogen-passivated silicon nanowires under ambient conditions, Chem. Mater. 17 (23) (2005) 5780–5788.

[176] E.M. Dibbern, F.J.J. Toublan, K.S. Suslick, Formation and characterization of polyglutamate core-shell microspheres, J. Am. Chem. Soc. 128 (20) (2006) 6540–6541.

[177] C. Christiansen, A.J. Vebner, B. Muan, H. Vik, T. Haider, H. Nicolaysen, T. Skotland, Lack of an immune response to Albunex, a new ultrasound contrast agent based on air-filled albumin microspheres, Int. Arch. Allergy Immunol. 104 (4) (1994) 372–378.

[178] A.E. Crawford, A practical introduction to ultrasonic cleaning, Ultrasonics 1 (2) (1963) 65–69.

[179] E. Macé, G. Montaldo, I. Cohen, M. Baulac, M. Fink, M. Tanter, Functional ultrasound imaging of the brain, Nat. Methods 8 (8) (2011) 662–664.

[180] S. Moon, L. Duchin, J.V. Cooney, Application of ultrasound to organic reactions: ultrasonic catalysis on hydrolysis of carboxylic acid esters, Tetrahedron Lett. 20 (41) (1979) 3917–3920.

[181] F. Touyeras, J.Y. Hihn, X. Bourgoin, B. Jacques, L. Hallez, V. Branger, Effects of ultrasonic irradiation on the properties of coatings obtained by electroless plating and electro plating, Ultrason. Sonochem. 12 (1–2) (2005) 13–19 (SPEC. ISS.).

[182] S. Mitragotri, Healing sound: the use of ultrasound in drug delivery and other therapeutic applications, Nat. Rev. Drug Discov. 4 (3) (2005) 255–260.

[183] R.R. Deshmukh, R. Rajagopal, K.V. Srinivasan, Ultrasound promoted C–C bond formation: Heck reaction at ambient conditions in room temperature ionic liquids, Chem. Commun. 17 (2001) 1544–1545.

[184] J.R. Askim, M. Mahmoudi, K.S. Suslick, Optical sensor arrays for chemical sensing: the optoelectronic nose, Chem. Soc. Rev. 42 (22) (2013) 8649–8682.

[185] K.R. Gopi, R. Nagarajan, Advances in nanoalumina ceramic particle fabrication using sonofragmentation, IEEE Trans. Nanotechnol. 7 (5) (2008) 532–537.

[186] K.S. Suslick, G.J. Price, Applications of ultrasound to materials chemistry, 2003.

[187] A. Kotlyar, N. Perkas, G. Amiryan, M. Meyer, W. Zimmermann, A. Gedanken, Coating silver nanoparticles on poly(methyl methacrylate) chips and spheres via ultrasound irradiation, J. Appl. Polym. Sci. 104 (5) (2007) 2868–2876.

[188] M. Rai, A. Yadav, A. Gade, Silver nanoparticles as a new generation of antimicrobials, Biotechnol. Adv. 27 (1) (2009) 76–83.

[189] D. Roe, B. Karandikar, N. Bonn-Savage, B. Gibbins, J. Baptiste Roullet, Antimicrobial surface functionalization of plastic catheters by silver nanoparticles, J. Antimicrob. Chemother. 61 (4) (2008) 869–876.

[190] D.M. Eby, H.R. Luckarift, G.R. Johnson, Hybrid antimicrobial enzyme and silver nanoparticle coatings for medical Instruments, ACS Appl. Mater. Interfaces 1 (7) (2009) 1553–1560.

[191] A. Kumar, P.K. Vemula, P.M. Ajayan, G. John, Silver-nanoparticle-embedded antimicrobial paints based on vegetable oil, Nat. Mater. 7 (3) (2008) 236–241.

[192] N. Perkas, G. Amirian, S. Dubinsky, S. Gazit, A. Gedanken, Ultrasound-assisted coating of nylon 6,6 with silver nanoparticles and its antibacterial activity, J. Appl. Polym. Sci. 104 (3) (2007) 1423–1430.
[193] a) K. Ghule, A.V. Ghule, B.-J. Chen, Y.-C. Ling, Preparation and characterization of ZnO nanoparticles coated paper and its antibacterial activity study, Green Chem. 8 (12) (2006) 1034;
b) P.K. Vabbina, A. Kaushik, N. Pokhrel, S. Bhansali, N. Pala, Electrochemical cortisol immunosensors based on sonochemically synthesized zinc oxide 1D nanorods and 2D nanoflakes, Biosens. Bioelectron. 63 (2015) 124–130.
[194] N. Vigneshwaran, S. Kumar, A.A. Kathe, P.V. Varadarajan, V. Prasad, Functional finishing of cotton fabrics using zinc oxide-soluble starch nanocomposites, Nanotechnology 17 (20) (2006) 5087–5095.
[195] J.R.G. Sander, B.W. Zeiger, K.S. Suslick, Sonocrystallization and sonofragmentation, Ultrason. Sonochem. 21 (6) (2014) 1908–1915.
[196] P. Wei, L. Yan, D. Linghu, Structure transformation induced in natural graphite during ultrasonic fragmentation, J. Mater. Sci. Lett. 17 (16) (1998) 1393–1394.
[198] L.A. Pérez-Maqueda, A. Duran, J.L. Pérez-Rodríguez, Preparation of submicron talc particles by sonication, Appl. Clay Sci. 28 (1–4) (2005) 245–255.
[199] S.-H. Jung, E. Oh, K.-H. Lee, W. Park, S.-H. Jeong, A sonochemical method for fabricating aligned ZnO nanorods, Adv. Mater. 19 (5) (2007) 749–753.
[200] Y. Wei, W. Wu, R. Guo, D. Yuan, S. Das, Z.L. Wang, Wafer-scale high-throughput ordered growth of vertically aligned ZnO nanowire arrays, Nano Lett. 10 (9) (2010) 3414–3419.
[201] S. Xu, Y. Wei, M. Kirkham, J. Liu, W. Mai, D. Davidovic, R.L. Snyder, Z.L. Wang, Patterned growth of vertically aligned ZnO nanowire arrays on inorganic substrates at low temperature without catalyst, J. Am. Chem. Soc. 130 (45) (2008) 14958–14959.
[202] B. Raeymaekers, C. Pantea, D. Sinha, Manipulation of diamond nano-particles using bulk acoustic waves, J. Acoust. Soc. Am. 128 (4) (2010) 2338.
[203] Y. Chen, C.L. Zhu, G. Xiao, Reduced-temperature ethanol sensing characteristics of flower-like ZnO nanorods synthesized by a sonochemical method, Nanotechnology 17 (18) (2006) 4537–4541.
[204] Y. Wei, Y. Li, N. Zhang, G. Shi, L. Jin, Ultrasound-radiated synthesis of PAMAM-Au nanocomposites and its application on glucose biosensor, Ultrason. Sonochem. 17 (1) (2010) 17–20.
[205] S. Myler, F. Davis, S.D. Collyer, S.P.J. Higson, Sonochemically fabricated microelectrode arrays for biosensors – part II: modification with a polysiloxane coating, Biosens. Bioelectron. 20 (2) (2004) 408–412.
[206] S. Mosadegh Sedghi, Y. Mortazavi, A. Khodadadi, Low temperature CO and CH_4 dual selective gas sensor using SnO_2 quantum dots prepared by sonochemical method, Sens. Actuators B Chem. 145 (1) (2010) 7–12.
[207] W. Guo, J. Yuan, E. Wang, Oligonucleotide-stabilized Ag nanoclusters as novel fluorescence probes for the highly selective and sensitive detection of the Hg^{2+} ion, Chem. Commun. (Camb.) (23) (2009) 3395–3397.
[208] Y.-F. Wang, J.-W. Li, Y.-F. Hou, X.-Y. Yu, C.-Y. Su, D.-B. Kuang, Hierarchical tin oxide octahedra for highly efficient dye-sensitized solar cells, Chem. Eur. J. 16 (29) (2010) 8620–8625 (S8620/1–S8620/4).
[209] J. Kim, K. Yong, A facile, coverage controlled deposition of Au nanoparticles on ZnO nanorods by sonochemical reaction for enhancement of photocatalytic activity, J. Nanopart. Res. 14 (8) (2012) 1–10.
[210] H.R. Liu, G.X. Shao, J.F. Zhao, Z.X. Zhang, Y. Zhang, J. Liang, X.G. Liu, H.S. Jia, B.S. Xu, Worm-like Ag/ZnO core–shell heterostructural composites: fabrication, characterization, and photocatalysis, J. Phys. Chem. C 116 (30) (2012) 16182–16190.
[211] L.J. Brennan, M.T. Byrne, M. Bari, Y.K. Gun'ko, Carbon nanomaterials for dye-sensitized solar cell applications: a bright future, Adv. Energy Mater. 1 (4) (2011) 472–485.
[212] J.H. Lee, J. Chang, J.H. Cha, Y. Lee, J.E. Han, D.Y. Jung, E.C. Choi, B. Hong, Large-scale, surfactant-free solution syntheses of $Cu(In, Ga)(S, Se)_2$ nanocrystals for thin film solar cells, Eur. J. Inorg. Chem. 5 (2011) 647–651.

Further reading

[197] Y. Wu, A. Bandyopadhyay, S. Bose, Processing of alumina and zirconia nano-powders and compacts, Mater. Sci. Eng. A 380 (1) (2004) 349–355.